The regulation of tyrosine hydroxylase by dopamine and selected binding partners

Master Thesis in Pharmacy

Gro Haugseng

Centre for Pharmacy and
the Department of Biomedicine

University of Bergen

May 2022

Summary

Tyrosine hydroxylase (TH) catalyses the rate limiting step in the metabolic pathway of dopamine (DA) synthesis and is therefore important in physiological functions such as motor control, cognitive function, and the brain reward system. DA is the main regulator of TH activity through feedback inhibition. The mechanism of this inhibition has recently been further elucidated, adding to the knowledge about the structure, regulation, and stabilization of TH through the inhibition by DA, which its reversed by Ser40 phosphorylation. An α-helix in the N-terminal of TH is especially important for the DA inhibition.

As DA levels are highly controlled, TH is regulated by several processes in addition to DA itself, notably by phosphorylation at different sites (Ser19, Ser31 and Ser40) and by several proteins that have been shown to regulate TH activity and stability. In this work, we have investigated the binding of three TH binding partners that have previously been shown to regulate TH, i.e. α-synuclein (α-syn), an abundant neuronal protein involved in vesicle trafficking, DNAJC12, the specific HSP40 co-chaperone of TH, and 14-3-3ζ, a regulatory phosphoprotein-binding protein that interacts with Ser19-phosphorylated (pSer19) TH. As the effect of these proteins on the binding of DA has not been previously investigated in detail, the aim of this work was therefore to study the interplay between the binding of these proteins on the inhibition of TH by DA. Furthermore, an additional aim in this thesis work was to characterize the complex formation between TH and α-syn.

Our initial binding studies, using the methods SEC-MALS, native-PAGE coupled with immunoblotting, crosslinking and Bio-layer interferometry (BLI), did not provide any insight regarding the interaction between TH and α-syn. Furthermore, our studies on the effect of TH regulatory proteins on DA binding and feedback inhibition, using BLI and enzymatic assays, suggested that DA and DNAJC12 can interact and regulate TH simultaneously, whereas DA and 14-3-3ζ mutually affects the interaction between pSer19 and its counterpart, likely due to the role of the N-terminal in both interactions.

Acknowledgments

The work presented in this master thesis was performed at the Martinez Lab, at the Department of Biomedicine at the University of Bergen from August 2021 to May 2022, under the guidance of Dr. Svein Isungset Støve, Prof. Aurora Martinez and PhD student Mary Dayne Sia Tai.

First and foremost, I would like to pay my special regards to my supervisors Dr. Svein Isungset Støve and Prof. Aurora Martinez for their invaluable input and encouragement throughout this project. I personally want to extend my gratitude to you for letting me take part in this project for my thesis year, and for making this an immensely educational and enjoyable experience.

I would also like to recognize the invaluable assistance of my co-supervisor PhD student Mary Dayne Sia Tai for aiding me in my practical lab work, as well as providing extremely useful feedback when turning my practical work into the words presented in this thesis paper.

I must also thank the members of Lab E for being such a welcoming and helpful group of people, and for providing such a positive work environment. Being part of this research group has given me insight into the field of Biomedicine; a basal but crucial step in the development of new clinical therapeutics.

A special thanks to my fellow Lab E master students, Inga Elise and Marthe, for sharing this experience with me.

I must also acknowledge Biocat and the Centre for pharmacy (UiB) for financial support to attend the NBS conference and present my work.

Finally, I would also like to extend my thanks to my family and friends for their unconditional love and support.

Gro Haugseng

May 2022

Table of contents

Abbreviations

Abbreviation	***Meaning***
AADC	Aromatic L-amino acid decarboxylase
α-syn	α-synuclein
BLI	Bio-layer interferometry
BSA	Bovine serum albumin
BH_4	Tetrahydrobiopterin
Cam	Chloramphenicol
DA	Dopamine
DTT	Dithiothreitol
EDC	1-ethyl-3-(3-dimethylaminopropyl)carbodiimide
EDTA	Ethylenediaminetetraacetic acid
HPLC	High performance liquid chromatography
IPTG	Isopropyl β-D-1-thiogalactopyranoside
Kan	Kanamycin
kDa	Kilodaltons
L-Dopa	L-3,4-dihydroxyphenylalanine
MBP	Maltose binding protein
NAC	Non-amyloid-β component
PD	Parkinson's disease
PPI	Protein-protein interaction
SEC	Size exclusion chromatography
Ser	Serine
Sulfo-NHS	N-hydroxysulfosuccinimide
TB	Terrific broth
TEV Protease	Tobacco etch virus protease
TH	Tyrosine hydroxylase
VMAT2	Vesicular monoamine transporter 2

1. Introduction

Tyrosine hydroxylase (TH) is an enzyme that, with the help of cofactors tetrahydrobiopterin (BH_4) and oxygen (O_2), converts L-Tyrosine to L-Dopa, the rate limiting step of the endogenous catecholamine biosynthesis pathway as illustrated in *Figure 1*. L-Dopa is further converted by a separate enzyme, the aromatic L-amino acid decarboxylase (AADC), to the catecholamine dopamine (1).

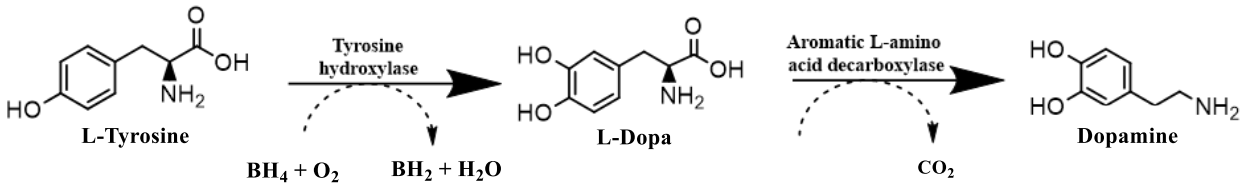

Figure 1: **The dopamine biosynthesis pathway.** The first step in the synthesis of dopamine, where L-Tyrosine is converted to L-Dopa, is catalysed by the iron (Fe^{2+}) dependent enzyme tyrosine hydroxylase (TH), using tetrahydrobiopterin (BH_4) as cofactor and molecular oxygen as additional substrate. The product, L-Dopa, is further processed by aromatic L-amino acid decarboxylase (AADC) to form dopamine.

Dopamine (DA) can then be further processed to produce norepinephrine and epinephrine and together, these catecholamines play important roles both as neurotransmitters in the central nervous system and as hormones in the neuroendocrine system (2). DA, in particular, plays an essential role in motor control, cognitive function and the brain reward system (3) and thus, the intracellular amount of DA must be tightly regulated. As illustrated in *Figure 2*, shortly after synthesis, DA is packed into vesicles that fuse with the membrane, releasing DA to the synaptic cleft. DA subsequently binds to receptors in the postsynaptic neuron, while the excess is transported back into the cytosol by reuptake transporters. When the concentration of DA increases in the cytosol, DA is degraded by monoamine oxidase or binds to TH and inhibits its enzymatic function, thus effectively decreasing the amount of available DA and suppressing further DA synthesis (4).

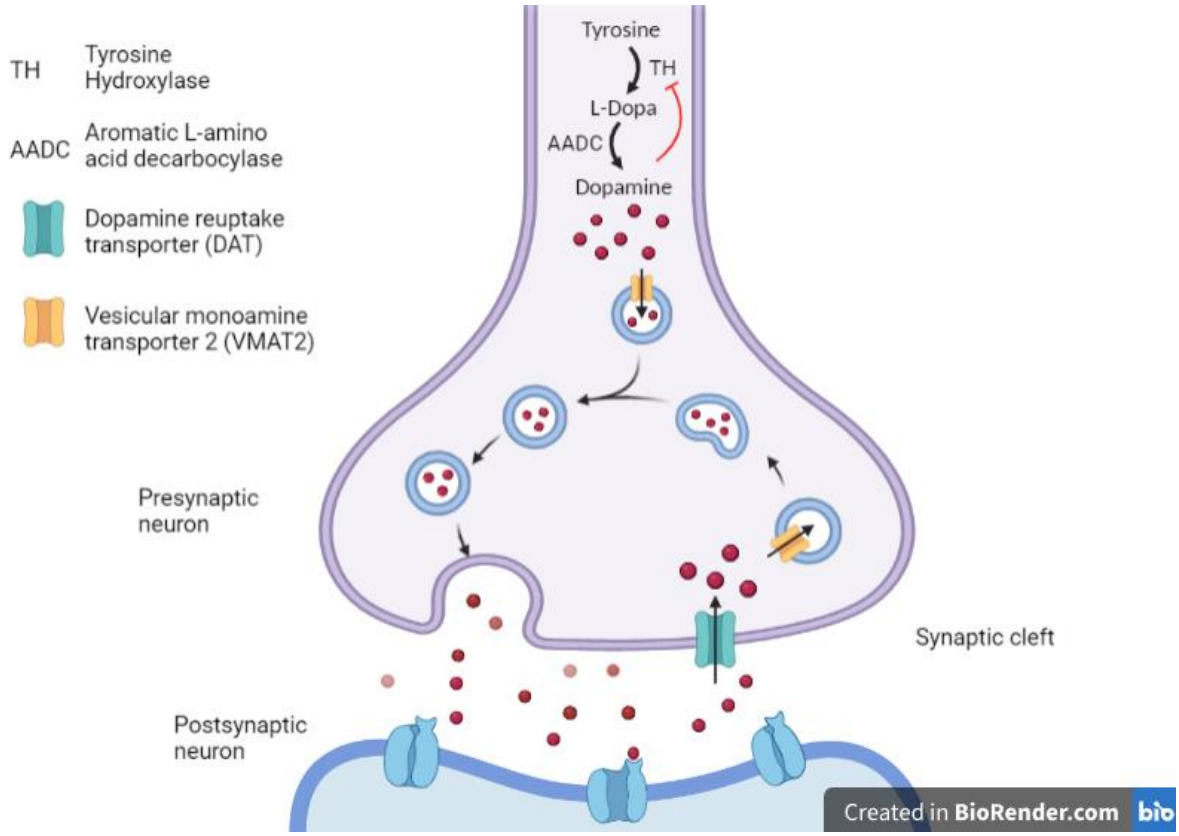

Figure 2: The dopamine signaling pathway. TH is the rate-limiting enzyme in dopamine (DA) synthesis, catalyzing the conversion of L-Tyrosine to L-Dopa. L-Dopa is further converted to DA by AADC. DA is packed into vesicles by VMAT2 and released into the synaptic cleft by exocytosis, before binding to DA receptors on the post-synaptic neuron. DA reuptake transporters remove DA from the synaptic cleft and transport it back into the cytosol, thus terminating the DA signal. With elevated levels of DA in the cytosol, DA binds to TH and inhibits the enzyme through a negative feedback mechanism that thus regulates further DA synthesis. *Created with biorender.com.*

1.1 Tyrosine hydroxylase

TH belongs to a family of enzymes known as the aromatic amino acid hydroxylases (AAAH), along with phenylalanine hydroxylase (PAH) and the tryptophan hydroxylases (TPH1 and TPH2). PAH is essential for the catabolism of phenylalanine and enzymatically converts L-Phenylalanine to L-Tyrosine, while the TPHs are key enzymes in the biosynthesis of serotonin by converting L-Tryptophan to 5-hydroxy-L-Tryptophan (5). Although the AAAHs serve different purposes *in vivo*, they are highly homologous homotetrameric enzymes that have a catalytic domain in each subunit (6, 7).

The human TH gene is made up of 14 exons and encodes for four isomers (hTH1, hTH2, hTH3, hTH4) from alternative splicing. The hTH1 isomer is the shortest and is made up of 497 amino

acids while hTH2, hTH3 and hTH4 have additions of 4, 27 and 31 amino acids respectively, between residues 30 and 31 in hTH1. The isomers hTH1 and hTH2 are the most abundantly expressed out of the four isomers, especially in brain, and the distribution of these isoforms varies between catecholaminergic neurones (8). In this thesis, all described experiments have been performed with hTH1, which will be referred to as TH WT from this point.

The dysfunction of TH has been associated with several diseases, as the abnormal activity of TH can lead to disruptions in the synthesis of DA, epinephrine, and norepinephrine. Mutations in TH have been particularly linked to the disease TH deficiency (THD), where patients present with DOPA-responsive dystonia or infantile parkinsonism of varying degrees (9) and, more recently, there has been increasing interest in the role of the enzyme in the neurodegenerative disorder Parkinson's disease, where TH and DA deficiency is observed in patients (5).

1.1.1 Structure of tyrosine hydroxylase

TH is a homotetrameric enzyme with a total molecular weight of 240 kDa. Each ~60 kDa subunit consists of a N-terminal regulatory domain spanning residues 1 to 165, a catalytic domain from residues 166 to 454, and a C-terminal oligomerization domain, from residues 455 to 497, as presented in *Figure 3A and B* (10). The isoform transcribed from the hTH1 gene has monomers of 55.6 kDa (11).

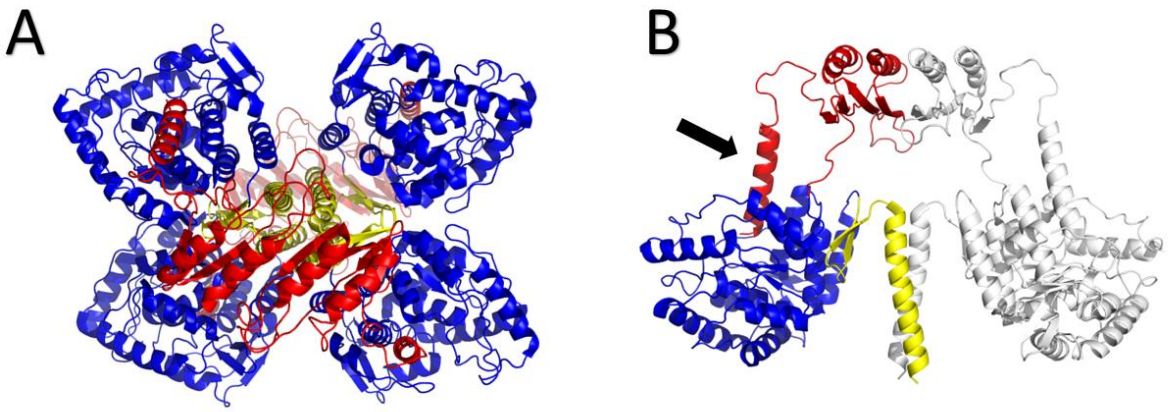

Figure 3: The atomic model of full-length TH in complex with dopamine (DA) (PDBID: 6ZVP) elucidated by cryogenic electron microscopy (cryo-EM) (5). TH is homotetramer, where each subunit is comprised of three domains: an N-terminal regulatory domain in red (residues 1-165), a catalytic core region in blue (residues 166-454) and a C-terminal tetramerization domain in yellow (residues 455-497). A) The full ~224 kDa tetrameric structure of TH. B) The structure of dimeric TH, containing two ~56 kDa monomeric units. The arrow points to the regulatory helix (residues 39-58), that blocks the active site upon DA binding.

The regulatory domain (RD) (*Figure 3*, coloured in red) consists of 165 amino acids and is the least conserved domain among the AAAHs. In the tetrameric structure of TH, the RDs form dimers, separated from the catalytic domains by 15 Å. This domain also plays an important part in the inhibitory feedback mechanism on TH by DA, in particular the 20 residue α-helical structure at position 39-58 of the N-terminal that blocks the active site of TH when bound to DA (5) (shown in *Figure 3B*). The RD harbours several phosphorylation sites that are important for regulating the activity of TH and plays an essential role in the inhibitory feedback mechanism of DA on TH, which will be described in more detail in Section 1.1.2.

The catalytic domain, on the other hand, is made up of 290 amino acids (*Figure 3*, coloured in blue) (7). As with all AAAHs, TH is dependent on the cofactors BH_4 and a non-heme iron (Fe^{2+}). The iron binds in the active site, to a 2-His-1-carboxylate facial triad (5), and is reduced to the active ferrous state by BH_4. The BH_4 binding site is well conserved between the AAAHs, but specific variations cause different conformations of the cofactor in the respective enzymes (12).

Finally, towards the C-terminal end of the protein lies an oligomerizaiton domain (*Figure 3*, coloured in yellow), a region that is 42 amino acids long and is involved in dimer and tetramer formation. The domain is made up of two β-strands, a loop and an α-helix that forms a coiled coil structure (13). Its structure includes two definite dimerization and tetramerization motifs (14) that

the subunits interact through to form a tetramer which is a dimer of dimers (10). The catalytic domain is also involved in the dimer formation, but the C-terminal alone is responsible for the tetramer formation (13).

1.1.2 Regulation of tyrosine hydroxylase

TH is mainly regulated by feedback inhibition of catecholamines that binds competitively with BH_4 to TH and through the phosphorylation of Serine (Ser) and Threonine (Thr) residues in the N-terminal regulatory domain of TH (8, 15). The binding of catecholamines affect the activity of TH through negative feedback, while regulation through phosphorylation can have an impact on enzymatic activity, localization and binding capacity to other proteins, depending on the site of phosphorylation (5).

The inhibition of TH activity by DA and other catecholamines occurs by the binding of these molecules to the N-terminal regulatory tail of TH. The binding of DA instigates a conformational change in the protein that results in the interaction of the 20 residue N-terminal α-helix (residues 39-58) to the binding site, locking DA in place and further strengthen the inhibition of TH activity. Upon phosphorylation of the Ser40 residue by cAMP-dependent protein kinase (PKA), the α-helix detaches from the binding site, allowing DA to dissociate, thus leading to the activation of TH (5).

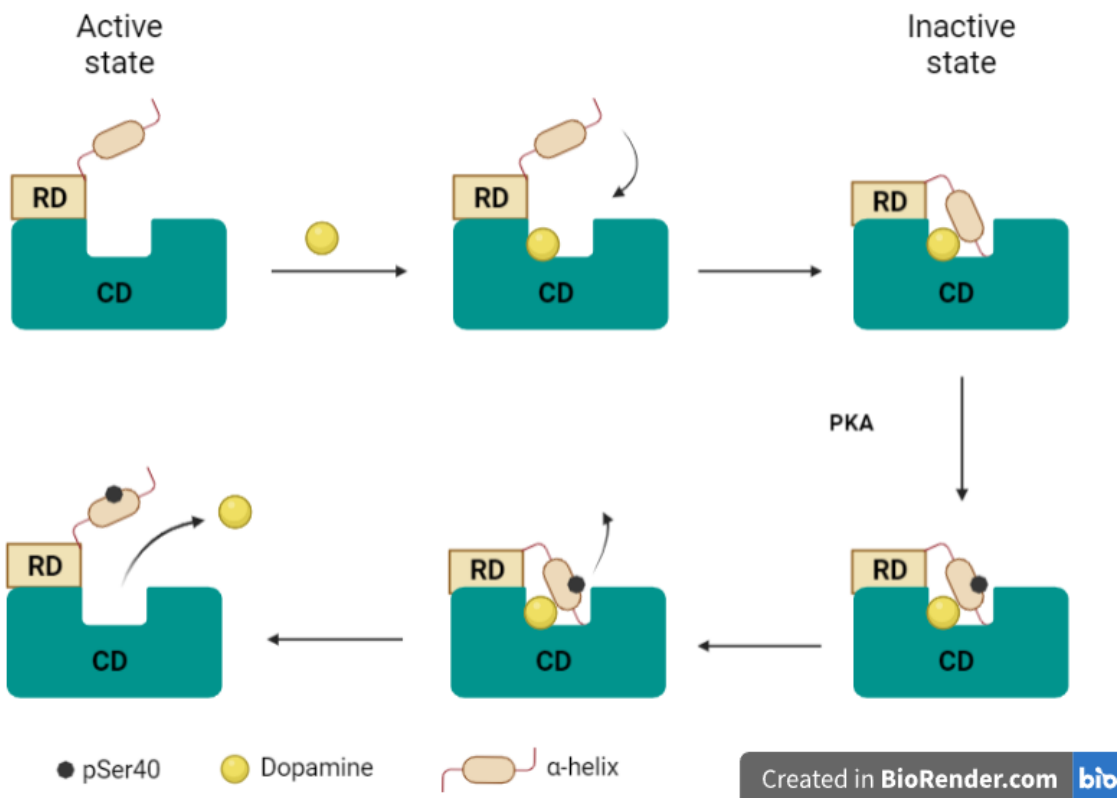

Figure 4: Feedback inhibition of TH by DA. DA binds to the active site of TH, initiating interaction of the α-helix (residues 39-58) of the regulatory domain (RD) with the catalytic domain (CD). DA is locked in the active site and TH inactivated. Upon phosphorylation of the Ser40 residue in the α-helix by PKA), the α-helix detaches from the CD and DA disassociates from the active site, leaving TH in its active state. Figure adapted from Bueno et al. (5). *Figure created with biorender.com*.

Phosphorylation of Ser and Thr residues, which is performed by various kinases specific to different N-terminal sites, is a post-translational modification (PTM) by which TH is also regulated. As mentioned above, the phosphorylation of the Ser40 residue plays an important role in TH activity by releasing the enzyme from the catecholamine feedback inhibition (5).

The phosphorylation at Ser31 (TH pSer31) influences the cellular localization of TH, as it has been shown that TH pSer31 is localized to the Golgi apparatus and vesicles (16). It has also been suggested that TH pSer31 could be transported from the cell body to the synaptic terminals *in vivo* and it has been shown to interact either directly or indirectly with the neuronal protein α-synuclein (α-syn) and the vesicular monoamine transporter 2 (VMAT2) *in vitro* (16).

Not much is known yet about the possible impact of Thr8 phosphorylation, while the phosphorylation of TH Ser19, on the other hand, is associated with binding to one of the known

binding partners of TH, 14-3-3. Previous studies using surface plasmon resonance have shown that phosphorylation of the Ser19 residue is vital for the stable interaction between TH and the 14-3-3ζ, an isoform very abundant in brain (17). Apart from using TH WT, several experiments in this thesis involve the use of several variants of TH to study the effects of phosphorylation on TH activity and binding, i.e. one where the serine residue in position 31 is exchanged for glutamic acid and another that has been phosphorylated *in vitro* at Ser19, which will be referred to as TH Ser31Glu and TH pSer19 respectively.

1.2 α-synuclein

α-synuclein (α-syn) is a neuronal protein that was first discovered in the electric organ of the Pacific electric ray (*Torpedo californica)* (18), as one of three forms of synuclein, named after their detected localization in the presynaptic terminal (syn) and the nucleus (nuclein). However, in later studies, it has been shown that α-syn is not located in the nucleus, and the previous detection of the protein in the nuclear envelope has been suggested to be caused by antibody contaminants (19). One of these synucleins was identified as α-syn in 1994 (20). Already in 1988, the synucleins were suggested to have a function in the coordination of synaptic events (18). Even though the function of α-syn is still not well understood, there is a general agreement that the protein contributes in the transport of vesicles as well as in synaptic vesicle exocytosis by binding to and facilitating soluble N-ethylmaleimide-sensitive factor attachment protein receptor (SNARE) complex assembly (21, 22).

α-syn is abundant in the brain, comprising up to 1% of the cytosolic proteins in the CNS (23), with high expression levels in the presynaptic terminals. α-syn has a monomeric molecular weight of 14 kDa (24), and its primary structure consists of 140 amino acids (25). The protein consists of 3 domains: an N-terminal which consists of α-helixes that binds to lipids or membranes, a core region also termed the non-amyloid-β component (NAC), and an acidic C-terminal tail. The N-terminal is made up of residues 1-60, the NAC region is comprised of residues 61-95, while the C-terminal spans residues 96-140 (25). In its monomeric state, the protein secondary structure is often described to possess a free unstructured conformation in the cytosol and while a more structured helical conformation is formed upon association with membranes (25, 26). α-syn also has a propensity to oligomerize and aggregate. The aggregation of several monomers leads to oligomers,

which can take on various forms. The accumulation of these abnormal forms of α-syn in neurons and glial cells has been associated with neurodegenerative diseases, collectively referred to as synucleinopathies, including Parkinson's disease (PD), multi system atrophy and Lewy body dementia (27). A common denominator for these diseases is the inclusion of aggregated α-syn into intracellular units. The form of these units varies to some degree between the different synucleinopathies and in PD and Lewy body dementia they are known as Lewy bodies (28). The misfolding and aggregation of α-syn is thought to be the primary cause for the death of dopaminergic neurons in PD (21). The NAC region of α-syn (residues, 61-95) has been shown to be important for the protein ability to aggregate, specially residues 71-82 (21, 29).

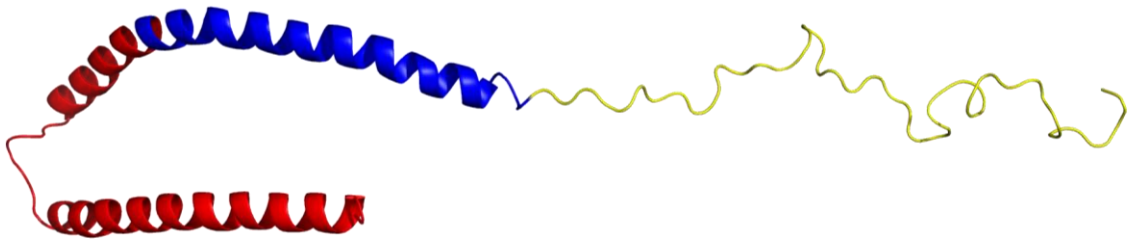

Figure 5: NMR structure of human micelle-bound alpha-synuclein (PDBID: 1XQ8) (30). Each domain of α-syn is illustrated by separate colours. The N-terminal Lipid binding domain in red (residues 1-60), the non-amyloid-β component (NAC) region in blue (residues 61-95) and the acidic C-terminal tail in yellow (residues 96-140).

An earlier study involving co-immunoprecipitation of rat brain homogenate has indicated that TH and α-syn interact *in vivo*, either directly or indirectly (31). Furthermore, the phosphorylation of TH at the Ser31 residue has been suggested to induce TH association with vesicles and transport from the cell soma to the terminals through interaction with α-syn and VMAT2 (16, 32). α-syn has been found to bind both iron and DA (33, 34) . The α-syn residue Glu83 and the C-terminal residues Tyr125-Ser129 are important for the binding of DA, that interacts with α-syn in a non-covalent, reversible manner (33). In addition, α-syn has been shown to reduce ferric iron (Fe^{3+}) to ferrous iron (Fe^{2+}) (34). Furthermore, earlier studies have suggested that α-syn could play a role in the regulation of the synthesis of DA, by reducing the activity of TH (31). This may indicate that α-syn could interact with the N-terminal domain of TH and thus potentially affect the inhibitory

feedback mechanism by DA on TH. It is therefore relevant to study the interaction of TH with and without DA, as well as the effect of DA on the interaction between TH and α-syn, to gain further insight in the regulation of TH.

1.3 DNAJC12

DNAJC12, previously known as J-domain containing protein 1 (JDP1), is a protein belonging to the heat shock protein 40 (HSP40) family, a group of proteins acting as co-chaperones for the members of the heat shock protein 70 (HSP70) family (35, 36). The HSP40s are also referred to as the DNAJ proteins, due to their characteristic J-domain (corresponding to residues 14-79 in DNAJC12) (35, 37), that includes the His-Pro-Asp motif that is essential for stimulating the intrinsic ATPase activity of HSP70s. As illustrated in *Figure 6*, the main function of HSP40s as co-chaperones is to recognize and bind to their specific clients, then transport them to the HSP70s. Together, the cooperation between HSP40 and HSP70 leads to client protein homeostasis through folding, refolding, degradation or aggregation prevention (35, 38).

The *DNAJC12* gene contains 5 exons that typically encode for a 198-residue protein, known as isoform a. A splice variant encoding a shorter isoform of DNAJC12 has also been reported, which contains only 107 amino acids (36). While both isoforms share the same N-terminal region, residues 1-99, the last eight residues of isoform b form an alternative sequence that is not found on isoform a. To this date, most studies have been carried out on the isoform a of DNAJC12. In this thesis, all described experiments have been performed with isoform a, referred to only as DNAJC12 from this point.

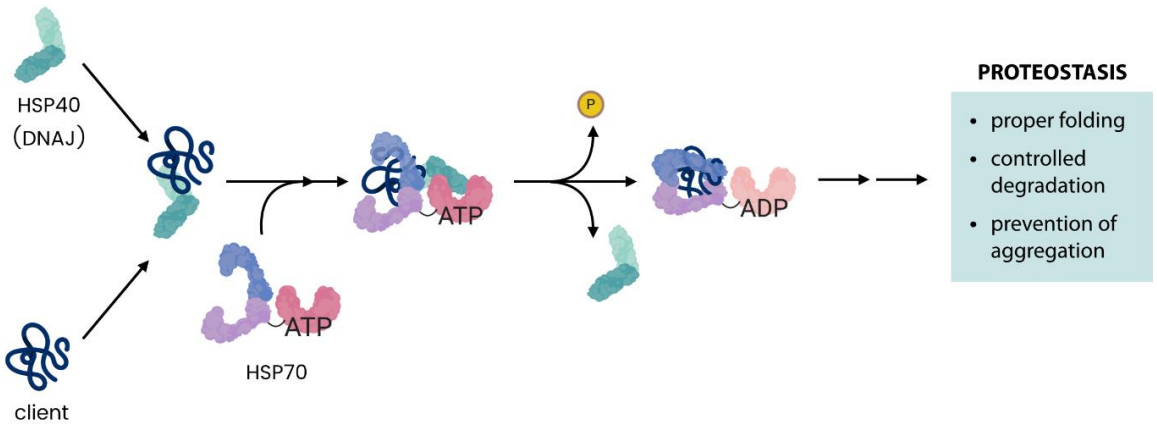

Figure 6: **The canonical DNAJ pathway**. HSP40/DNAJ co-chaperones interact with its client and guides it to the HSP70 chaperone to aid in proper folding, controlled degradation and aggregation prevention (39).

DNAJ proteins also contain other motifs, in addition to the J domain, allowing them to interact with other cellular proteins (36). DNAJC12 has been shown to interact and contributes to maintain the intracellular folding and functional levels of AAAHs PAH, TH, TPH1 and TPH2, which appear as the specific clients of DNAJC12 (35). It is thus expected that the interaction of DNAJC12 with TH aids in maintaining their homeostasis in the cell. Apart from this, it has been previously shown that DNAJC12 is able to stabilize TH by delaying its time-dependent self-aggregation *in vitro* (*Figure 7)* (39). However, the molecular mechanisms behind DNAJC12 and TH binding, as well as the exact biological consequences of this interaction still remain unclear.

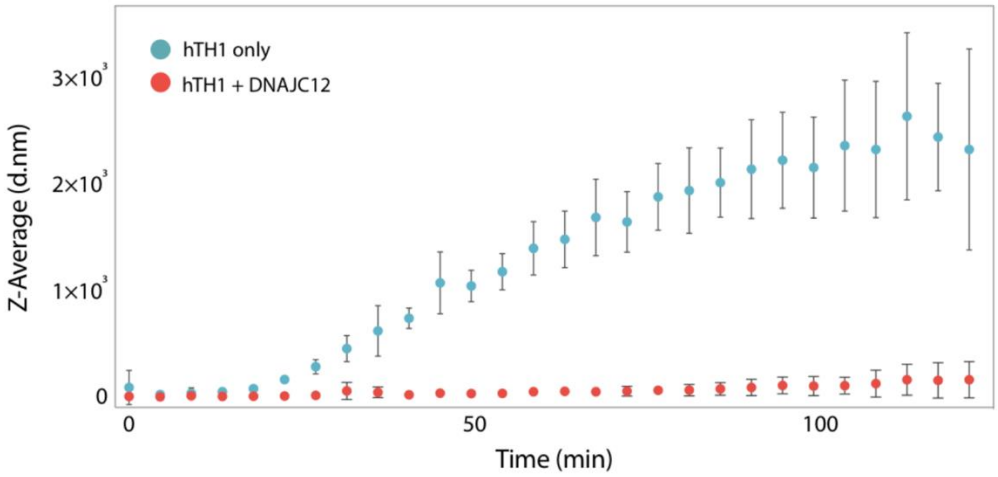

Figure 7: The interaction of DNAJC12 with TH slows down aggregation of the enzyme. The aggregation of TH monitored in the presence (red) or absence (blue) of DNAJC12 by dynamic light scattering **(39).**

Prior to 2017, DNAJC12 was mainly recognized pathogenically in association to several cancer types, as it was observed to be upregulated in cancers such as subtypes of colorectal and gastric cancers, as well as in triple negative breast cancer (40-42). However, in 2017, DNAJC12 was discovered to play a role in hyperphenylalaninemia (HPA), diseases causing accumulation of L-phenylalanine. HPAs are formerly recognized for their association with PAH and cofactor BH_4 deficiencies, but DNAJC12 deficiency is now also acknowledged as a cause for HPA (35, 37). Apart from HPA, these patients also presented with dopamine and serotonin deficiencies typical of dysfunctional TH and TPH (35). Thus, it is crucial to understand the mechanisms behind the interaction between DNAJC12 and its clients in order to elucidate the pathogenic mechanisms behind DNAJC12 deficiency.

1.4 14-3-3ζ

In 1980, a rat brain protein was isolated and acknowledged as an activator of the AAAHs TH, TPH1 and TPH2 (43). This activator protein was later discovered to be very similar to the bovine brain 14-3-3 protein, and shown to share both physicochemical and immunochemical characteristics (44). In later years, the 14-3-3 proteins have also been recognised for their contribution in a number of processes, such as the regulation of cell cycle, metabolism, apoptosis, and gene transcription (17).

There are seven mammalian 14-3-3 protein isoforms (β, γ, ε, η, ζ, σ, and τ/θ), a family of acidic regulatory proteins (17, 45). The seven isoforms differ in structure and the difference might be related to their respective substrate specificities. The various isoforms are also found distributed differently in cellular compartments (46). The 14-3-3 proteins, apart from the σ-isoform, exist both as homo- and hetero- dimers. Structurally, each monomer includes nine antiparallel helixes. These helices are involved in dimerization and the formation of amphipathic grooves important for ligand binding (17, 45, 47). Each dimer possesses two of these amphipathic binding pockets and thus has the ability to interact concurrently with two binding partners (48).

Upon binding, 14-3-3 regulates the binding partner through several mechanisms such as altering the conformation of the binding partner, impacting its activity or stability, e.g. by masking protein surface characteristics and aiding protein-protein complex formation (17). 14-3-3 binding to target proteins is often dependent on, and in consequence regulated by, phosphorylation (48). The interaction between TH and 14-3-3 proteins is regulated by Ser19 phosphorylation (TH pSer19) (2). The requirement for phosphorylation is strict and cannot be mimicked by Ser19Glu or Ser19Asp mutagenesis (Dr. Rune Kleppe, personal communication). The 14-3-3 proteins bind to TH pSer19, as illustrated in *Figure 6* (2). The figure shows the crystal structure for 14-3-3γ bound to the 1-43 residue N-terminal TH peptide, phosphorylated at the Ser19 residue. The binding of 14-3-3 proteins to TH is suggested to be induced by a conformational change in the N-terminal region surrounding the Ser19 residue, brough forward by phosphorylation in this position (2). 14-3-3ζ, the selected isoform in this work due to is abundance in brain (17) ,likely interacts with the N-terminal of TH in a similar manner (49) .

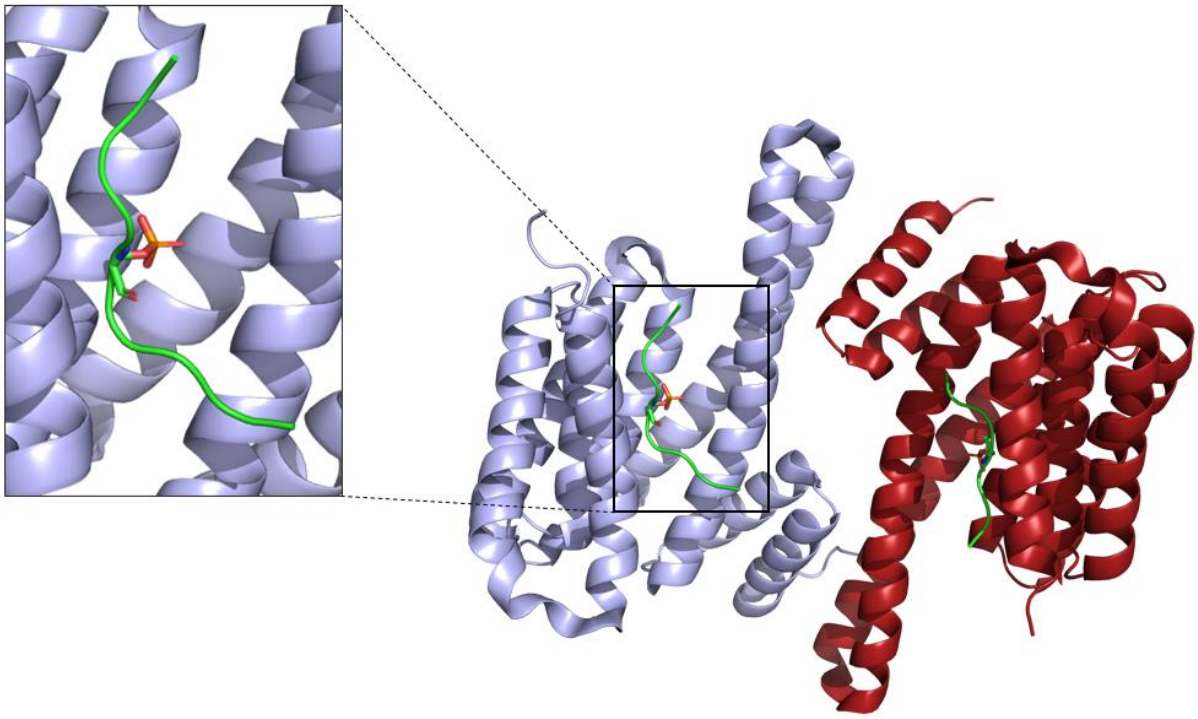

Figure 8: Crystal figure of 14-3-3γ complexed with the N-terminal sequence of tyrosine hydroxylase (residues 1-43) with a phosphorylated Ser19 (PDB ID: 4J6S) (2).

As the 14-3-3 proteins take part in a variety of cellular processes, they have also been associated with several diseases including Alzheimer's disease, PD and cancer. In Alzheimer's disease, the 14-3-3 proteins appear to be downregulated (50). Additionally, isomers ζ, ε, γ and σ, have been detected in Lewy bodies. The 14-3-3 proteins have also been shown to share sequence homology with α-syn, which also is found in Lewy bodies (45). The 14-3-3ζ isoform in particular has appeared in several cancer research reports (51), and its overexpression has also been reported in cancer types such as breast (52), lung (53) and pancreatic cancer (54).

2. Aims

The enzyme tyrosine hydroxylase (TH) catalyses the rate limiting step of the synthesis of dopamine (DA), and is thus crucial for many physiological functions, such as motor control, cognitive function, and the brain reward system. TH is highly regulated, and the master regulator of TH activity and stability is DA, which modulates TH through an inhibitory feedback mechanism. TH has also been shown to directly interact with DNAJC12 and 14-3-3 proteins and reported to associate with α-syn on synaptic vesicles and in co-immunoprecipitation experiments, but whether TH and α-syn form a stable protein-protein complex has yet to be shown.

As the mechanism of DA feedback mechanism has been recently elucidated at the structural level (5) the *primary objective of this thesis* was to investigate the interplay between the interaction of TH with the selected regulatory proteins α-syn, DNAJC12 and 14-3-3ζ and the feedback inhibition by DA, and interpret the effects based on the structure of DA-bound TH. Furthermore, an additional aim on this thesis has also been to characterize the complex formation between TH and α-syn at the molecular level.

3. Materials and Methods

3.1 Chemicals and reagents

Chemical	Supplier
2-Propanol	VWR chemicals
Acetic acid > 99.8 %	Sigma Aldrich
Agar-Agar	Merck
Ammonium iron(II) sulfate hexahydrate ($(NH_4)_2Fe(SO_4)_2*6H_2O$)	Sigma Aldrich
Ampicillin	Sigma Aldrich
Bovine Serum Albumin	Sigma Aldrich
Benzamidine hydrochloride hydrate	Sigma Aldrich
Calcium chloride-dihydrate ($CaCl_2*2H_2O$)	Merck
Catalase	Sigma Aldrich
Chloramphenicol	Sigma Aldrich
Disodium hydrogen phosphate (Na2HPO4)	Sigma Aldrich
DL-Dithiothreitol	Sigma Aldrich
Ethanol	Sigma Aldrich
Ethylenediaminetetraacetic acid	Thermo Fischer
EZ-Link™ NHS-PEG4-Biotin	Thermo Scientific
Glucose	Sigma Aldrich
Glycerol	Sigma Aldrich
Glycine	Sigma Aldrich
HEPES	Sigma Aldrich
Imidazole	Sigma Aldrich
Isopropyl-Beta-D-Thiogalactopyranoside (IPTG)	Apollo Scientific
Kanamycin	Sigma Aldrich
LB Broth (Lennox)	Sigma Aldrich
L-Tyrosine	Sigma Aldrich
Magnesium chloride hexahydrate ($MgCl_2*6H_2O$)	Merck
Magnesium sulphate ($MgSO_4$)	Sigma Aldrich
Paraformaldehyde (PFA)	Alfa Aesar
Potassium Chloride (KCl)	Sigma Aldrich
Potassium phosphate dibasic trihydrate ($K_2HPO_4*3H_2O$)	Sigma Aldrich
Potassium phosphate monobasic (KH_2PO_4)	Sigma Aldrich
Phosphate-buffered saline tablet	Sigma Aldrich
Sodium chloride (NaCl)	Merck
Sodium dodecyl sulfate (SDS)	Sigma Aldrich

Tetrahydrobiopterin	Schircks Laboratories
Tobacco Etch Virus Protease	Purified in Lab E
Trizma Base	Sigma Aldrich
Tryptone/ Peptone	Merck
Tween 20	Sigma Aldrich
Yeast extract	Sigma Aldrich

3.2 Expression and purification of recombinant proteins

In this work I expressed and purified TH wild type (TH WT), the phospho-mimicking variant TH Ser31Glu and α-syn. The other proteins studied in this thesis, DNAJC12 and 14-3-3ζ, as well as TEV protease, were expressed and purified and gently provided by other members of the Martinez lab. TH WT, TH Ser31Glu and α-syn were expressed by recombinant expression, a method involving the transfer of a plasmid that contains the open reading frame encoding the target protein to a bacterial cell, through a process called transformation.

The plasmids transformed into the bacteria also confer resistance to antibiotics and can thus be used to select successfully transformed cells. The pETMBP1a/*hTH1* plasmid encoding for TH variants *(Figure 9A)* included a kanamycin (kan) resistance gene, while the pET21a-*alpha-synuclein* plasmid included an ampicillin (amp) resistance gene *(Figure 9B).* The proteins were also expressed with a fusion tag to increase solubility and to ease purification. The TH variants were fused with an N-terminal 6xHistidine (His) and maltose binding protein (MBP) tag, while α-syn was fused only with a N-terminal 6xHis tag.

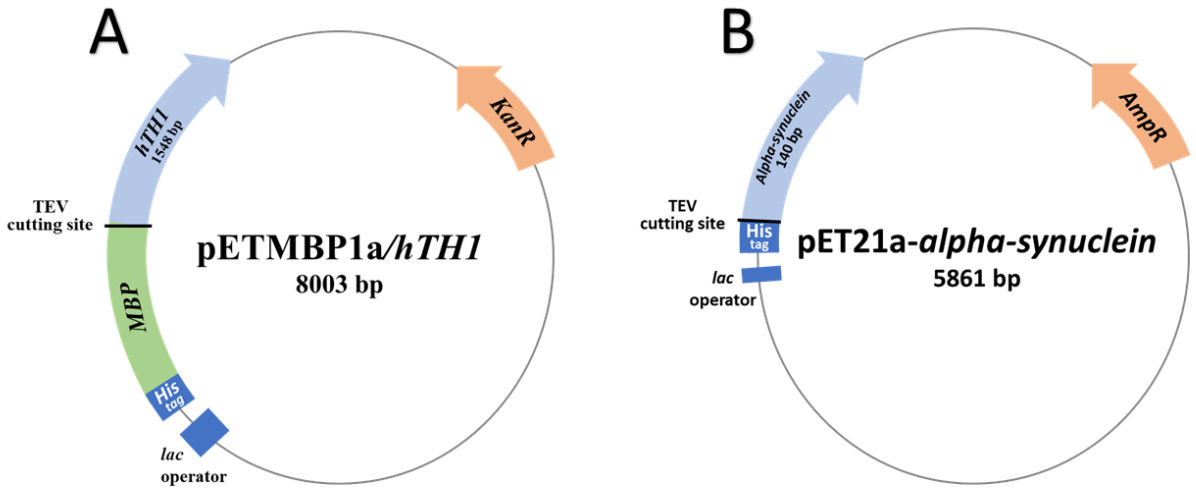

Figure 9: Simplified plasmid maps for pETMBP1a/*hTH1* and pET21a-*alpha-synuclein*. A) The open reading frame for the His-MBP-TH fusion protein and kanamycin resistance (*KanR*) are shown as arrows. The TEV cutting site and lac operator are also shown in the figure. B) The open reading frame of the His-alpha-synuclein fusion protein and ampicillin resistance (*AmpR*) are shown as arrows. The TEV cutting site and lac operator are also shown in the figure.

3.2.1 Expression of tyrosine hydroxylase

His-MBP-TH WT and His-MBP-TH Ser31Glu were expressed in *E. coli* BL21 Codon Plus competent cells (Agilent Technologies) using the pETMBP1a/*hTH1* plasmid prepared by Bezem, et al (1) and the pETMBP-1a/*hTH Ser31Glu* plasmid prepared by Kråkenes (55), respectively, using the same expression protocol (1). Transformed cells containing the respective plasmids were inoculated in 25 mL Terrific Broth (TB) media supplemented with 50 µg/mL kan and 34 µg/mL chloramphenicol (cam), then incubated at 28 ^{o}C overnight with shaking (200 rpm). The cultures were then diluted in TB media (1 L) with the same concentration of kan and cam and incubated at 37 ^{o}C with shaking (200 rpm) until the cultures reached an optical density at 600 nm (OD_{600}) of 1.2. To induce protein expression, 0.5 mM IPTG was added to the culture and supplemented with 100 mg of ammonium iron (II) sulfate hexahydrate before overnight incubation at 20^{o}C with shaking (200 rpm). The cultures were harvested by centrifugation (20 min, 4 ^{o}C, 4500 x g) and the cell pellet was washed by resuspension in cold PBS (25 mL) and centrifugation (20 min, 4 ^{o}C, 4500 x g). Washed cell pellets were stored at -80 ^{o}C.

3.2.2 Purification of tyrosine hydroxylase

The purification of TH WT and TH Ser31Glu was performed through a two-step purification protocol. The first step includes cell lysis and affinity chromatography. Bacterial cells were lysed by sonication to extract the soluble proteins, the insoluble fraction and cell debris were removed by centrifugation and the fusion protein was then purified from the cell lysate by affinity chromatography.

Affinity chromatography is a method where molecules with high affinity for the purification resin is separated from other components in the sample. The molecules with affinity for the resin are retained in the column, whilst the other components pass through. For the TH fusion proteins, we used amylose resin that will bind to the MBP tag. The fusion proteins were eluted with maltose which has a higher affinity to the MBP and will outcompete binding to the amylose resin.

In the second purification step the purified TH fusion proteins were cut with tobacco etch virus (TEV) protease to remove their fusion partners, and the products were separated by size exclusion chromatography (SEC). TEV cuts the fusion protein at the TEV recognition site between the tag

and the protein, as shown in *Figure 9*. The sequence of the TEV recognition site is ENLYFQS, and the TEV protease cuts the sequence between Q and S.

SEC is a method that separates molecules based on their size. The resin used for this method has pores of specific sizes, that small molecules can diffuse into, whilst larger molecules are excluded. Small molecules will therefore be held back, while the larger molecules move faster through the column. The larger molecules such as TH (~56 kDa) thus elute earlier than the smaller molecules such as His-MBP (45 kDa) and TEV (28 kDa).

The bacterial pellets were resuspended in 5-10 mL of lysis buffer (20 mM HEPES, 20 mM NaCl, 10 mM benzamidine, 1 cOmplete EDTA-free tablet (Roche) per 30 mL) per gram of pellet, then further lysed (cells disrupted) by sonication for 3 x 45 sec (9 sec pulse, output 20 W) using a Vibra-Cell™ Ultrasonic Liquid Processor (Sonics & Materials, Inc.). The lysate was centrifuged (20 min, 20 000 x g, 4 °C) to remove cell debris.

The supernatant was collected and diluted 1:1 with binding buffer (20 mM HEPES, 200 mM NaCl, pH 7), before running through pre-equilibrated amylose resin on an XK column (GE Healthcare) connected to an ÄKTAprime plus system to obtain the fusion protein. The column was then washed with binding buffer, until an OD_{280} of less than 0.08 was reached. The protein was eluted from the column with the binding buffer supplemented with 10 mM maltose. The eluate was collected and concentrated using 50K MWCO Amicon® Ultra-15 Centrifugal Filter Units (Merck Millipore).

The concentration of the fusion protein was measured using a NanoDrop™ One^c Microvolume UV-Vis Spectrophotometer (Thermo Scientific) using the theoretical extinction coefficient (ε) of 1.1 (1 mg/mL) (11), and stored in liquid nitrogen until further purification steps.

To remove the affinity tag, TEV, was added to the sample in a 1:10 TEV:protein ratio and incubated at 4 °C for 1-2 h. Tetrameric TH was then isolated by SEC. The TEV-cutting mix was separated on a HiLoad 16/600 s200 column (GE Healthcare) connected to the ÄKTA pure system (GE Healthcare). The fractions containing tetrameric TH were selected, pooled and concentrated using 50K MWCO Amicon® Ultra-15 Centrifugal Filter Units. The concentration of the final purified protein was measured on the NanoDrop™ One^c Microvolume UV-Vis Spectrophotometer using the theoretical extinction coefficient (ε) of 0.73 (1 mg/mL) (11) and stored as aliquots in liquid

nitrogen. Samples from each purification step were collected and analysed using sodium dodecyl sulfate – polyacrylamide gel electrophoresis (SDS-PAGE) as described in Section 3.3.

3.2.3 Expression of α-synuclein

To prepare α-syn, single colonies of *E. coli.* BL21 Star™ containing the pET21a-*alpha-synuclein* plasmid prepared by M. Jakubec et al. (56) were inoculated at 27 °C overnight, in TB media (25 mL) with a concentration of 100 µg/mL amp. The following morning, the cultures were diluted in TB (0.5 L) with the same concentration of amp and incubated at 37 °C in orbital shakers (200 rpm). Protein expression was induced by adding IPTG to a final concentration of 0.1 mM at OD_{600}=0.4, and cell cultures harvested by centrifugation (10 000 x g, 20 min, 4 °C) 5 h later. Pellets were washed by resuspension in cold PBS (25 mL), centrifuged again (4500 x g, 20 min, 4 °C) and the pellet stored at -80 °C.

3.2.4 Purification of α-synuclein

The purification of the recombinant α-syn is performed through several steps. The bacterial cells are first lysed by osmotic shock to extract the soluble proteins and the fusion protein is then purified from the cell lysate by immobilized metal affinity chromatography (IMAC).

For the His-α-syn fusion protein, we used TALON® resin that has high affinity to the His-tag. The fusion protein was eluted with imidazole which outcompetes the his-tag from the resin, due to the higher affinity of imidazole for the cobolt-ion in the resin.

The purified fusion protein was then cut with TEV protease to remove the fusion partner, and α-syn separated from the cleavage products by reverse IMAC. In the last step of the purification, α-syn was separated from larger oligomers and other unspecific binders from IMAC by SEC.

The bacterial pellets were lysed with 20 mL osmotic shock buffer (30 mM Tris, 2 mM EDTA, 40% sucrose, pH 8) per gram of pellet and incubated at room temperature for 10 min. The cells were harvested by centrifugation (3900 xg, 20 min, 4 °C) and resuspended in 45 mL of cold 1 mM $MgCl_2$. The lysate was centrifuged (20 000 x g, 20 min, 4 °C) and the supernatant was

collected and supplemented with two cOmplete, EDTA-free Protease Inhibitor Cocktail tablets (Roche) and Na_2HPO_4 to a final concentration of 20 mM.

Immobilized metal affinity chromatography (IMAC) was performed to obtain the fusion protein. The crude extract was loaded onto a HiTrap (5 mL) pre-packed column (Cytiva) connected to the ÄKTAprime plus system (GE Healthcare) pre-equilibrated with running buffer (20 mM Tris, 150 mM NaCl, pH 8). The column was subsequently washed with washing buffer until an $OD_{280} < 0.08$ was reached. The protein was then eluted out from the column by the elution buffer (20 mM Tris, 150 mM NaCl, 250 mM imidazole, pH 8), collected and concentrated using 10K MWCO Amicon® Ultra-15 Centrifugal Filter Units (Merck Millipore) until a volume of approximately 500 µL was reached. The concentrated eluate was re-diluted with washing buffer and concentrated again, until the theoretical concentration of imidazole was below 0.1 mM.

The concentration of the fusion protein was measured with on the NanoDrop™ One^c Microvolume UV-Vis Spectrophotometer (Thermo Scientific) using the theoretical extinction coefficient (ε) of 0.390 (1 mg/mL) (11), then supplemented with TEV in a 1:50 protease:fusion protein ratio to remove the fusion tag. The mix was also supplemented with EDTA and DTT to a final concentration of 0.5 mM and 1 mM respectively, prior to overnight incubation at 4 ^oC.

Cleaved α-syn was separated from cleaved His tags, uncleaved His- α-syn and TEV by reverse IMAC using TALON resin (TaKaRa Bio) in a gravity column. The column was pre-equilibrated with running buffer (20 mM Tris, 150 mM NaCl, pH 8) prior to the addition of the mix to the column. The flow-through from washing with 3 column volumes of running buffer was then collected and concentrated using the 10K MWCO Amicon® Ultra-15 Centrifugal Filter Units (Merck Millipore).

The concentrated sample was loaded onto a Superdex 75 Increase 10/300 GL column (GE Healthcare) on an ÄKTA pure system (GE Healthcare) for SEC. The fractions containing α-syn were collected and concentrated using the 10K MWCO Amicon® Ultra-15 Centrifugal Filter Units (Merck Millipore). The concentration of the purified product was measured using the NanoDrop™ One^c Microvolume UV-Vis Spectrophotometer (Thermo Scientific) with the theoretical extinction coefficient (ε) of 0.412 (1 mg/mL) (11), and stored as aliquots in liquid nitrogen.

3.3 Sodium dodecyl-sulfate polyacrylamide gel electrophoresis (SDS-PAGE)

Sodium dodecyl-sulfate polyacrylamide gel electrophoresis (SDS-PAGE) is a method used to separate proteins in a mixture based on their molecular weight. Prior to electrophoresis, the proteins are denatured by the addition of the reducing agent dithiothreitol (DTT) and by exposure to heat. The samples are also prepared in a buffer containing SDS that coats the proteins in a uniform negative charge, thus causing the proteins to migrate by mass. This method was thus used to assess the quality and purity of the purified proteins.

The samples were first diluted 1:1 in 2x Laemmli sample buffer (62.5 mM Tris-HCl, pH 6.8, 2% SDS, 25% glycerol, 0.01% bromophenol blue, and 100 mM DTT added fresh prior to use), heated for 5 min at 95°C on an Eppendorf Thermoblock and loaded onto a Mini-PROTEAN® TGX™ Precast Gel (Bio-Rad) in a Mini-PROTEAN® Tetra cell (Bio-Rad) with running buffer (25 mM Tris, 192 mM glycine, 0.1% SDS, pH 8.3). A Precision Plus Protein™ dual color standard (Bio-Rad) was added as a reference for the molecular weights of the respective proteins. The gel was run at 200 V for approximately 25 min. To visualize the protein bands, the gel was stained using Coomassie (0.08 mM Coomassie brilliant blue G-250 (Bio-Rad), 5 mM HCl), destained in water and imaged using the ChemiDoc XRS+ System (Bio-Rad).

3.4 Native PAGE

Polyacrylamide gel electrophoresis under native conditions (native PAGE) is a method used to separate proteins in their native state. Unlike in SDS-PAGE, the samples are not denatured with heat, SDS and the reducing agent DTT, and thus retain their native state. The migration of the proteins is therefore mainly driven by their size, shape, and overall charge. This method was used to study the possible complex formation between TH and α-syn. The samples contained 3.6 μM TH WT or TH Ser31Glu and 14.3 μM α-syn. The respective controls each held 3.6 μM TH, 3.6 μM TH Ser31Glu or 14.3 μM α-syn. The samples and controls were diluted 1:1 with native sample buffer (62.5 mM Tris-HCl, pH 6.8, 40% glycerol, 0.01% bromophenol blue) and loaded onto a 4-15% Mini-PROTEAN® TGX™ Precast Gel (Bio-Rad) in a Mini-PROTEAN® Tetra cell (Bio-Rad) with native PAGE running buffer (25 mM Tris, 192 mM glycine, pH 8.3). The samples were then subjected to electrophoresis at 140V for 4 h at 4 ^{o}C. After the electrophoresis, the gel was

either stained with Coomassie as explained in Section 3.3 or transferred to a PVDF membrane for western blot analysis as explained in section 3.5.

3.5 Immunoblotting

Western blot, or immunoblotting, is a method for detecting distinctive proteins in a sample. This analysis was performed to detect α-syn in samples and evaluate complex formation. Proteins are first separated by either SDS-PAGE or native PAGE then transferred onto a membrane. The membrane is then treated with a primary antibody that binds to a specific epitope on a targeted protein and subsequently with a secondary antibody that binds the primary antibody and allows the protein to be detected by chemiluminescence.

The proteins were transferred to a polyvinylidene difluoride (PVDF) membrane using a Trans-Blot® Turbo™ Transfer System (Bio-Rad) and a Trans-Blot Turbo Mini 0.2 µm PVDF Transfer Pack. The transfer was run at a current of 2.5 A and a voltage of 25 V, for 3 and 5 min, respectively, for the SDS-PAGE gel analysis and the Native-PAGE gel analysis. Before immunodetection, the membrane was soaked in paraformaldehyde (PFA) for 30 min to fix the proteins to the membrane, washed with PBS-T (0.01 M phosphate buffer, 0.0027 M potassium chloride, 0.137 M sodium chloride, 0.1 % Tween 20, pH 7.4) for 5 min and then soaked in blocking buffer (5% dry milk w/v in washing buffer) for 1 h at room temperature to limit unspecific binding. The primary antibody, anti-α-synuclein (D37A6) Rabbit mAb (Cell Signaling Technology, cat#4179), was added to the blocking buffer at a ratio of 1:1000, then incubated with gentle agitation for 1 h at room temperature or overnight at 4 °C. Afterwards, the membrane was washed in PBS-T for 10 min three times and incubated with the secondary antibody, goat anti-rabbit pAb conjugated to horse radish peroxidase (Bio-Rad, cat#170-6515), at a ratio of 1:5000 in a solution of 3% dry milk in PBS-T for 1 h at room temperature. The membrane was washed again for 10 min three times in PBS-T and for 5 min in PBS. Finally, the membrane was treated with approximately 100 µL of Immobilon Crescendo Western HRP substrate (Millipore) per cm^3 of membrane area prior to visualization with the Bio-Rad ChemiDoc™ XRS+ system.

3.6 Bioactivity assays of tyrosine hydroxylase

A bioactivity assay, or enzymatic assay, is a method used to evaluate the effect of one or more compounds on the activity of an enzyme. In this study, bioactivity assays were performed to investigate the effects of selected TH binding partners on the inhibitory feedback mechanism of DA on TH.

The bioactivity assays were performed at 37 ºC on an Eppendorf thermoblock with variable reaction conditions. Standard 50 µL reaction mixes were prepared to contain 1 µg/mL TH, 40 mM HEPES, 0.1 mg/mL catalase, 10 µM Fe $(NH_4)_2Fe(SO_4)_2*6H_2O$), 50 µM L-Tyrosine and 200 µM BH_4. TH was added to samples containing HEPES, catalase, Fe, L-tyrosine and optionally dopamine, α-syn, DNAJC12 and/or 14-3-3ζ. These assay samples were then incubated at 37 ºC for 1 minute, before the reaction was started by adding BH_4. After a set time, the reactions were stopped by adding 50 µL of 2% (v/v) acetic acid in ethanol. The samples were then placed in the -20 ºC freezer for 90 min to allow protein precipitation. The amount of L-Dopa in the supernatant of each reaction was then quantified by high-performance liquid chromatography (HPLC) with a Zorbax 300-SCX column (Agilent Technologies) attached to a 1200 series high performance liquid chromatography (HPLC) system (Agilent technologies). The chromatographic separation was obtained with a mobile phase containing 20 mM Hac, 1% propanol, pH 3.5, at a flow rate of 2 ml/min. Two L-Dopa standards that contained 9.9 µM DOPA + 12,5 µM L-Tyrosine and 5 µM L-DOPA respectively were prepared to calibrate for L-Dopa measurements.

3.6.1 Binding partners of tyrosine hydroxylase and their effect on dopamine inhibition

To assess the effect of different binding partners on the inhibitory feedback mechanism of DA on TH, assays were performed in the presence and absence of a selection of TH binding partners, and a concentration gradient of dopamine (100, 50, 25,12.5, 6.25, 3.13, 1.56, 0.78, 0.39, 0.20, 0.10, 0.05, 0.02 and 0 µM) to determine the DA concentration needed to inhibit 50% TH activity, i.e. the IC-50 value, at the different assay conditions. The concentration of each binding partner remained the same throughout the assays: 0.021 µM DNAJC12, 0.009 µM DNAJC12 (when added in complex with TH), 5 µM α-syn and 0.054 µM 14-3-3ζ.

3.7 SEC-MALS

SEC-MALS was performed using a Superdex™200 Increase 10/300 GL connected to the Shimadzu HPLC coupled to a RefractoMax 520 module (ERC, Inc.) and mini-DAWN TREOS detector (Wyatt). The column was equilibrated with 20 mM HEPES, 200 nM NaCl, pH 7.0 prior to sample analysis at a flow rate of 0.50 mL/min. For binding studies, a sample containing 20 μM of TH and 80 μM of α-syn was used for the experiment. Samples containing only 20 μM TH or only 80 μM were used as controls. Prior to analysis, the samples were filtered using Corning® Costar® Spin-X® (0.22 μM) plastic centrifuge tube filters (Merck). Sample molar masses were estimated using the Astra software (Wyatt).

3.8 Crosslinking protein interaction analysis

A crosslinking reaction is the process of chemically joining two or more molecules by a covalent bond using crosslinkers that activate specific functional groups for binding. The crosslinker N-hydroxysulfosuccinimide (sulfo-NHS) activate carboxyl-groups and the crosslinker 1-ethyl-3-(3-dimethylaminopropyl)carbodiimide (EDC) activate a primary amine group. Sulfo-NHS and EDC can be combined to form ester bonds more efficiently. Crosslinking experiments were performed in an attempt to strengthen the bond between TH and α-syn.

The crosslinking reaction was performed by mixing 4 mM sulfo-NHS and 10 mM EDC, then adding proteins to the mix. 80 μM α-syn was mixed with 20 μM TH WT or 20 μM TH Ser31Glu to observe crosslinking between the proteins. Crosslinking reactions containing 80 μM α-syn, 20 μM TH WT or 20 μM TH Ser31Glu alone were also prepared as controls. The crosslinking reactions were incubated for 30 min at room temperature in the dark then subsequently analysed by SDS-PAGE.

3.9 Bio-Layer Interferometry (BLI)

Bio-Layer Interferometry (BLI) experiments were performed to measure the affinity and kinetics of the interaction between TH and its respective binding partners, with and without the presence of DA. BLI is a method based on the interference pattern of white light reflected off a biosensor.

In BLI experiments, a biotinylated molecule is immobilized to a streptavidin biosensor, due to the strong interaction between biotin and streptavidin. The biosensor with the immobilized protein is then dipped into a solution containing the presumed binding partner. Binding the sensor will cause a shift in the interference pattern of the white light reflected, which is measured in real time and can be analysed.

3.9.1 The interaction between tyrosine hydroxylase and α-synuclein

Prior to the studies on the effect of DA on the affinity between TH and binding partners, a test experiment was performed for the interaction between TH WT and α-syn. Phenylalanine hydroxylase (PAH) was also immobilised to the sensor and allowed to interact with α-syn as a negative control.

To prepare for the BLI analysis, the first step was to biotinylate TH WT and PAH. A buffer exchange was first performed on TH WT, using Zeba spin desalting columns (Thermo Scientific) following the manufacturer's protocol. EZ-Link™ NHS-PEG4-Biotin (Sigma Aldrich) and TH WT were mixed at a molar ratio of 1.5:1 and incubated for 30 min at room temperature. The excess biotin was then removed using another round of buffer exchange.

The binding samples were prepared by exchanging the buffer of α-syn to 1X PBS, then preparing a solution of 300 μM α-syn in the reaction buffer (1X PBS with 0.5 mg/mL Bovine serum albumin (BSA), 0.02% Tween 20). Biotinylated TH WT and TH pSer19 was also diluted to 0.05 mg/mL in the reaction buffer and 200 μL of each of the samples were loaded to their respective wells. For this experiment, we used streptavidin (SA) biosensors (Sartorius) and were soaked in 1X PBS for at least 1 h prior to the analysis.

The BLI analysis was performed using the Octet Red96 system (ForteBio) at 25 ^{o}C with the assay steps defined in *Table 1*. When there is binding, one expects to see a stable baseline, an increasing signal when loading the biotinylated protein, a stable baseline after loading, an increasing signal that stabilizes after a given time during the association step, then a decrease in signal at the dissociation step.

TABLE 1: The BLI analysis was carried out in the five steps listed below at a temperature of 25 ºC.

Step type	Step type	Sample type	Duration (s)
Sensor check	Baseline	Buffer	30
Loading	Loading	Biotinylated protein	300
Baseline	Baseline	Buffer	120
Association	Association	Binding partner	600
Dissociation	Dissociation	Buffer	300

3.9.2 The effect of dopamine on the affinity between tyrosine hydroxylase and binding partners

Further experiments were performed to test the effect of DA on the interaction between TH and DNAJC12, and TH pSer19 and 14-3-3ζ. TH WT and TH pSer19 was prepared for the BLI-analysis by biotinylation as explained in section 3.8.1. The binding samples were made by first exchanging the buffer of DNAJC12 or 14-3-3ζ to 1X PBS, then by preparing a concentration series of DNAJC12 (2000, 1000, 500, 100, 10 nM) and 14-3-3ζ (5000, 1000, 500, 100, 10 nM), respectively, in the reaction buffer (1X PBS with 0.5 mg/mL bovine serum albumin (BSA), 0.02% Tween 20). Biotinylated TH was also diluted to 0.05 mg/mL in the reaction buffer and 200 µL of each of the samples were loaded to their respective wells. For this experiment, we used streptavidin (SA) biosensors (Sartorius), which were soaked in 1X PBS for at least 1 h prior to the analysis. The BLI analysis was performed using the Octet Red96 system (ForteBio) at 25 ºC with the assay steps defined in *Table 1*. The assay between TH WT and DNAJC12 without DA shown in *Figure 18A* was kindly performed by Mary Dayne Sia Tai.

3.10 Statistical analysis

Statistical analysis was performed for the data collected from BLI, enzymatic assays and SEC-MALS. The results from SEC-MALS were estimated using the Wyatt ASTRA software. The K_d-values obtained from the BLI-assays were calculated using nonlinear regression (curve fitting) and presented as the mean with standard error of the mean (mean ± SEM) of three repeated experiments. The enzymatic assays were performed with three replicates, and the results are calculated using nonlinear regression (curve fitting) and reported as the mean with standard error of the mean (mean ± SEM) of two repeated experiments. The IC50- and K_d-values respectively were compared and analyzed to determine the statistical significance of the IC50-values (differences were deemed significant when $p<0.05$). All statistical analyses were performed using an extra sum-of-squares F test of the best fit values in GraphPad prism version 9.

4. Results

4.1 Expression and purification of recombinant proteins

4.1.1 Expression and purification of His-MBP-tyrosine hydroxylase fusion proteins

To investigate protein-protein interactions between TH and its potential binding partners, as well as their effect on the inhibitory feedback mechanism of DA on TH, we recombinantly expressed and purified TH WT and TH Ser31Glu from *E. coli* BL21-CodonPlus bacteria to enable *in vitro* studies on the proteins. The competent cells were first transformed with the pETMBP1a/*hTH1 or* pETMBP1a/*hTH1 Ser31Glu* plasmids and grown in TB media. *Figure 10A,B* shows the SDS-PAGE analysis of TH WT and TH Ser31Glu cultures, respectively, before and after the induction of protein expression with IPTG. In both cases, as we expected, a band corresponding to the His-MBP-TH fusion protein was observed in the sample with IPTG, but not in the sample taken prior to induction with IPTG. The size of the bands is approximately 100 kDa, which is consistent with the theoretical sizes of the His-MBP-TH fusion proteins (96 kDa) (11).

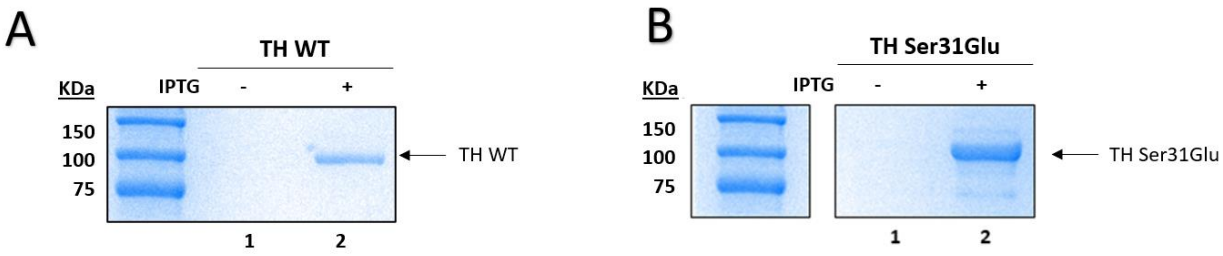

Figure 10. Expression of TH fusion proteins. A) SDS-PAGE analysis before and after expression of TH WT induced with IPTG, confirming expression of TH WT. B) SDS-PAGE analysis before and after expression of TH Ser31Glu induced with IPTG, confirming expression of TH Ser31Glu. Both gels follow the same loading scheme. Lane 1: uninduced culture; lane 2: induced sample using 0.5 mM IPTG. The Precision Plus™ Dual Color Standard was used as a molecular weight ladder.

The bacterial cells were harvested by centrifugation and lysed by sonication to prepare for purification. The His-MBP-TH fusion proteins were first separated from the other components in the lysate by affinity chromatography using amylose resin. The yields of fusion protein were 29.4 mg per litre of culture for TH WT and 23.8 mg per litre for TH Ser31Glu. The purified fusion protein was then cleaved with TEV protease to separate TH from its fusion partner. In the final purification step, TH was separated from TEV, its fusion partner, and from other impurities by

SEC. The resulting chromatograms for both the WT and variant form of TH contain three peaks: a small peak of early elution products that most likely corresponds to larger oligomers, a second peak corresponding to the elution of the TH tetramers, and a peak likely accounting for other cleavage products such as TEV and the His-MBP tag (*Figure 11A and 11B*).

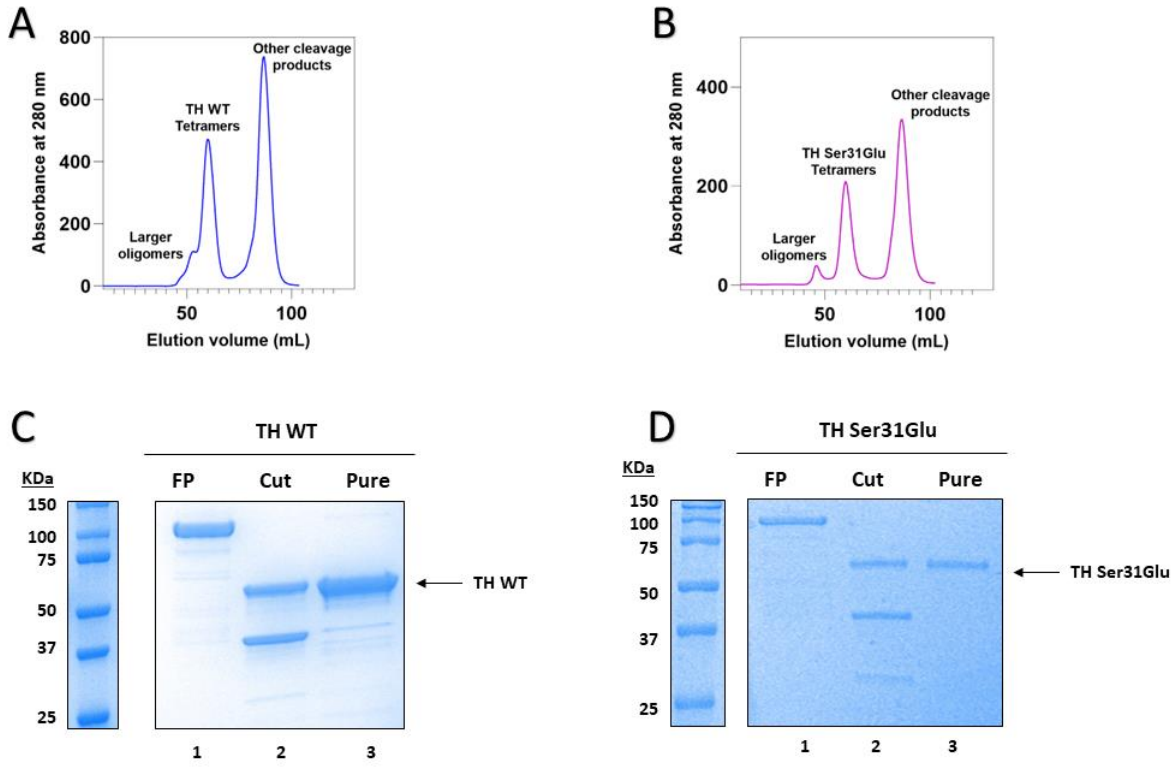

Figure 11: Purification of TH WT and TH Ser31Glu. A) Chromatogram of the cut His-MBP-TH WT fusion protein and B) His-MBP-TH Ser31Glu showing the separation of larger oligomers, TH WT tetramers and other cleavage products such as TEV protease and His-MBP on a HiLoad™ 16/60 Superdex™ 200 PG column at 4°C at 1 mL/min. C) Denaturing SDS-PAGE gel analysis of TH WT and D) TH Ser31Glu samples. Lane 1: fusion protein; lane 2: cut fusion protein; lane 3: pure TH. The Precision Plus™ Dual Color Standard was used as a molecular weight ladder.

Interestingly, when performing SEC, despite TH WT (55.6 kDa) and TH Ser31Glu (55.7 kDa) (11) having approximately the same molecular weight the proteins eluted at slightly different volumes. The proteins eluted at 60.03 mL and 59.88 mL, with the phospho-mimicking variant eluting slightly earlier than WT TH as shown in *Figure 11A* and *Figure 11B*. The same phenomenon has been observed by Trond-André Kråkenes in his work with the initial purification of TH Ser31Glu (55), and has been suggested to be due to a conformational change imparted by the phospho-mimic residue to the protein that results in a slightly larger conformation that ultimately leads to its earlier

elution. After SEC, 8.5 mg of tetrameric TH WT and 7 mg of tetrameric TH Ser31Glu were obtained from 29.4 mg and 23.8 mg of the fusion protein respectively.

Samples from each purification step were analysed by SDS-PAGE, as shown in *Figure 11C and 11D*. In lane 1 of both figures, which contains samples of the purified fusion proteins of wildtype and mutant TH respectively, a strong band at approximately 100 kDa was observed, in agreement with their theoretical size of 96 kDa (11). In lane 2 of both gels, we observe three bands, at approximately 60 kDa, 40 kDa and 30 kDa. These bands agree with the expected bands for TH WT or TH Ser31Glu with a theoretical size of ~56 kDa (11), His-MBP with a theoretical size of 43 kDa, and TEV with a theoretical size of 27 kDa. In lane 3, mainly the band at ~60 kDa is visible, corresponding well with the ~56 kDa size of TH. These results confirmed the purity of the isolated protein, and the proteins were stored as aliquots in liquid nitrogen until further use.

4.1.2 Expression and purification of α-synuclein

α-syn was recombinantly expressed and purified from *E. coli* BL21-Star bacteria to enable *in vitro* studies with the protein. The competent cells were transformed with the pET21a-*alpha-synuclein* plasmid and grown in TB media prior to the induction of protein expression with IPTG. α-syn cultures samples prior to, and after the addition of IPTG were collected and analysed by denaturing SDS-PAGE *(Figure 12)*. A weak band at approximately 18 kDa can be observed in the induced sample (lane 2), that is not present in the uninduced sample (lane 1), which is consistent with the 17 kDa theoretical size of the His-α-syn fusion protein (11).

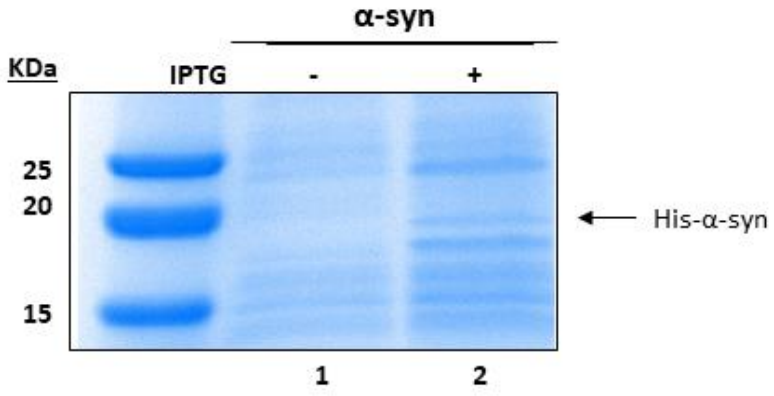

Figure 12: Expression of α-syn. SDS-PAGE analysis of cultures before and after the induction of protein expression with IPTG, verifying the expression of α-syn. Lane 1: uninduced culture; lane 2: induced culture with 0.1 mM IPTG. The Precision Plus™ Dual Color Standard was used as a molecular weight ladder.

While the band corresponding to the α-syn fusion protein was weak, it still denoted the successful expression of the protein, albeit the probability of lower protein yields. Thus, the bacterial cultures were harvested by centrifugation and lysed by osmotic shock to prepare for purification. The His-α-syn fusion protein was first separated from the other components in the lysate by affinity chromatography with a HiTrap (5 mL) pre-packed column, resulting in approximately 10 mg of fusion protein. The purified fusion protein was then cleaved with TEV protease to remove the fusion tag. After cleavage, the protein was separated from its fusion partner and His-tagged TEV protease by reverse IMAC with TALON® resin and was further purified through SEC, yielding 1.4 mg of pure α-syn.

The resulting chromatogram of α-syn *(Figure 13B)* using SEC on showed that the protein eluted at 9.90 mL, as shown in *Figure 13A***.** α-syn elutes earlier than one would expect, which could suggest it had aggregated or formed oligomers. However, as shown in *Figure 14B*, it was confirmed by SEC-MALS that α-syn elutes as a monomer. This was also observed by Trond-André Kråkenes in his work when purifying α-syn. It was then noted that α-syn eluted earlier than the control protein MBP (~40 kDa), and that the early elution was likely due to the unstructured nature of α-syn (55, 57).

Samples from each purification step were also analysed by SDS-PAGE to assess the purity of the purified α-syn, as shown in *Figure 13B*. In lane 1, containing the purified fusion protein, a single band was observed at approximately ~19 kDa, in agreement with the theoretical size of His-α-syn which is 17 kDa. Upon analysis of the cut sample, a single band was also observed at ~18 kDa, running slightly further down the gel than the fusion protein, consistent with the removal of the short His tag. Unlike with the purification of TH where bands corresponding to TEV protease and His-MBP were detected, no other bands were detected in the cut sample for α-syn, as the His-tag and the TEV protease was removed from the mix by reverse IMAC.

After further purification of the sample, a single band was observed at ~18 kDa corresponding well with the theoretical size of α-syn (14 kDa). The purity of the protein was thus confirmed using SDS-PAGE *(Figure 13B)* and SEC-MALS *(Figure 14B)*, and the protein was stored as aliquots in liquid nitrogen until use in further experiments.

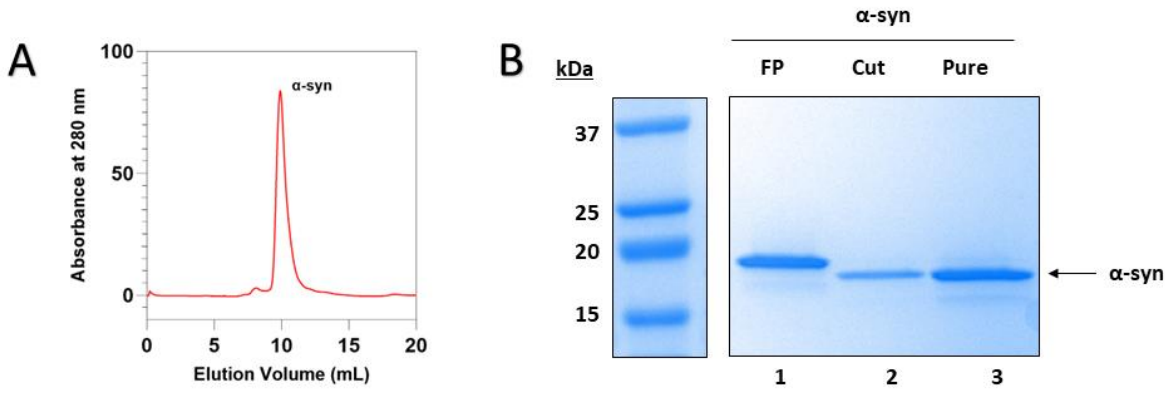

Figure 13: Purification of α-syn. A**)** SEC elution profile of the cut His-α-syn fusion protein, showing the separation of larger oligomers and the target protein on a Superdex™ 75 10/300 column at 4°C and 0.5 mL/min flow rate. B**)** SDS-PAGE gel analysis of samples collected at different stages of purification. Lane 1: α-syn fusion protein; lane 2: TEV-cut fusion protein; lane 3: purified α-syn. The Precision Plus™ Dual Color Standard was used as a molecular weight ladder.

4.2 Investigating the complex formation between α-synuclein and tyrosine hydroxylase

To investigate the interaction between TH and α-syn, purified recombinant proteins were first analysed together by SEC-MALS. Native PAGE analysis coupled with immunoblot was also performed to study the possible comigration of TH and α-syn through a gel.

4.2.3 SEC-MALS

As an initial experiment to investigate the formation of the TH: α-syn complex, the purified recombinant TH and α-syn proteins were analysed together and separately by SEC-MALS. Analysis of TH alone through SEC-MALS *(Figure 14A)* shows a single population that elutes at approximately 11 mL, that has a size of 218 kDa ± 0.7%, consistent with the theoretical size of tetrameric TH (224 kDa). Similarly, the analysis of purified α-syn using the same technique also resulted in a single peak eluting at ~14.5 mL *(Figure 14B)*. Despite being a 14 kDa protein, α-syn eluted early from the Superdex™ 200 10/300. However, as expected, SEC-MALS estimated the size of the protein to be 15 kDa ± 8.2%, consistent with the theoretical size of monomeric α-syn.

A sample containing both TH and α-syn was also analysed using SEC-MALS to determine whether the two proteins could bind and elute together in a single peak. However, our results (*Figure 14C*) show that this sample contains two separate populations that elute out at ~11 mL and ~14.5 mL respectively, consistent with our results with tetrameric TH (*Figure 14A*) and monomeric α-syn (*Figure 14B*). Indeed, the proteins eluting out in these peaks were sized at 220 kDa ± 0.1% and 15 kDa ± 5.2%, demonstrating that while the two proteins were present in the sample they did not elute together as a complex, which indicates that most probably they do not bind, and if they do the binding affinity is very low. As can be seen in *Figure 14D*, by overlapping all three chromatograms, there was no difference in the elution profile of TH in the presence or absence of α-syn in the sample.

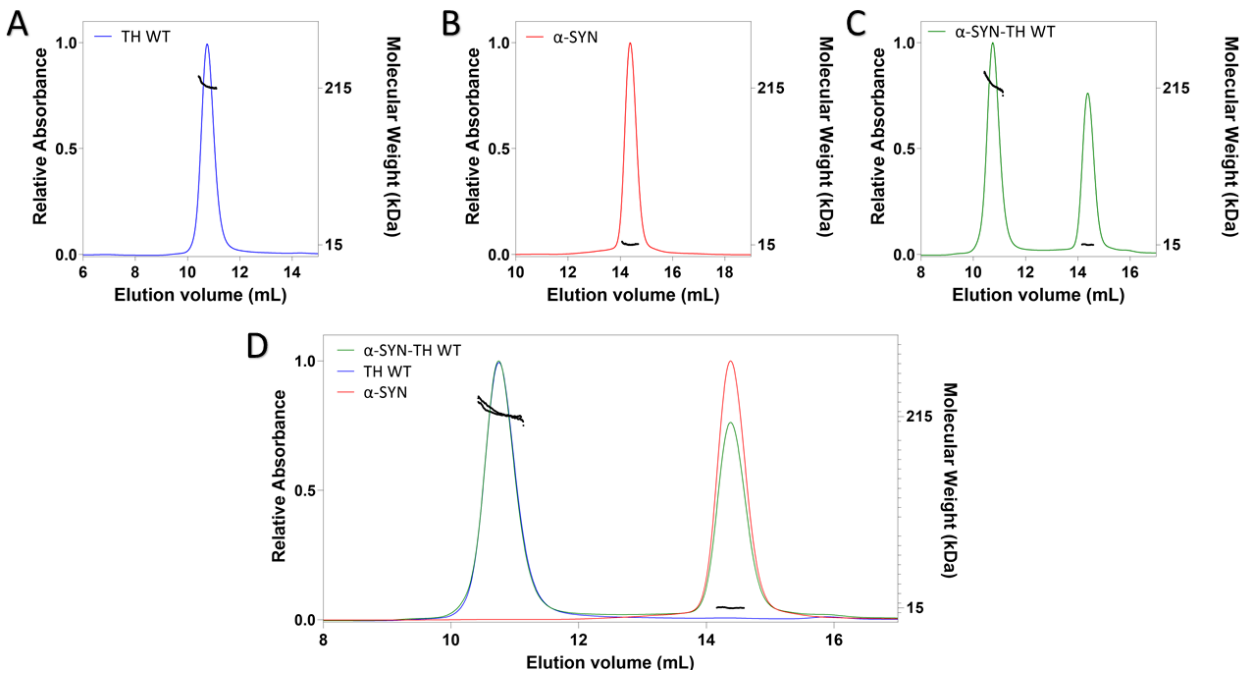

Figure 14: Analysis of TH WT: *α*-syn complex formation by SEC-MALS. Individual elution profiles and molecular weight analyses (black) of A) TH WT alone (blue), B) α-syn alone (red) and C) α-syn and TH WT together (green) on a Superdex™ 200 10/300 column at 4°C and 0.5 mL/min flow rate. D) An overlay of the three graphs and their respective molecular weight signals showing that there was no change in the size of TH in the presence of α-syn.

4.2.1 SDS-PAGE, Native-PAGE, and Western blot

Samples containing both TH WT and α-syn were analysed by SDS-PAGE and Native PAGE, followed by subsequent Coomassie staining or immunoblotting, to investigate the poorly defined interaction between the two proteins. While the two techniques are similar, the main difference between Native PAGE and SDS-PAGE is that while SDS-PAGE is an analysis of fully denatured protein samples which all have the same negative charge-protein size ratio, the native state of a given protein sample is retained in the non-denaturing conditions on a Native PAGE analysis, and separation of the proteins in the gel is based not only on protein size, but also overall protein charge. This allows us to study protein complexes by Native PAGE gel electrophoresis, and by mixing the two proteins and retaining their native state, we hope to detect the presence of a species that migrates slower through the gel than unbound tetrameric TH due to increased size of a protein complex. An SDS-PAGE analysis of the same samples is also performed in parallel to verify the presence of all components of each sample. In addition, to achieve an increased sensitivity of

detection, immunoblotting was done for both denaturing and non-denaturing conditions to identify the presence of α-syn in the samples. The resulting immunoblots and Coomassie stained gels are shown in *Figure 15A* for the SDS-PAGE and in *Figure 15B* for the Native-PAGE analyses respectively. Both immunoblots were performed using antibodies against α-syn.

As expected, in lane 2 of *Figure 15A*, which was loaded with TH WT, a band was observed at ~60 kDa in the Coomassie stained gel, but not in the immunoblot, confirming the presence of TH in the sample, but not α-syn. In lane 3, which contains α-syn, a band is present at ~17 kDa in the Coomassie-stained gel, which is also detected by the anti- α-syn antibodies by western blotting, consistent with the theoretical size of the loaded α-syn control. In the sample containing both TH WT and α-syn (lane 4), two bands were observed at ~60 kDa and ~17 kDa on the Coomassie stained gel, agreeing with the theoretical sizes of TH WT and α -syn proteins, both loaded in this lane**.** Taken together, the results from the SDS-PAGE analysis and the subsequent immunoblotting indicate the correct loading of proteins for the Native PAGE analysis.

In *Figure 15B*, which displays the results obtained from Native PAGE and subsequent immunoblotting, lane 1 is loaded with TH WT, which appears on the Coomassie stained gel, but not detected in the immunoblot, as expected. As expected in lane 2, which contains the α-syn control, a single band is observed and detected in both the Coomassie stained gel and the immunoblot. Lastly, in lane 3 where TH WT and α-syn were loaded together, two strong bands were detected by Coomassie staining, corresponding to both unbound TH and α-syn. A very light band can be observed with a slower migration than unbound tetrameric TH in the gel, which could indicate the formation of a complex. However, only one band is detected in the immunoblot of the same sample using antibodies against α-syn, which migrates quickly through the gel and corresponds to unbound α-syn. This suggests that the proteins have migrated separately, and therefore does not indicate a direct interaction between the two proteins.

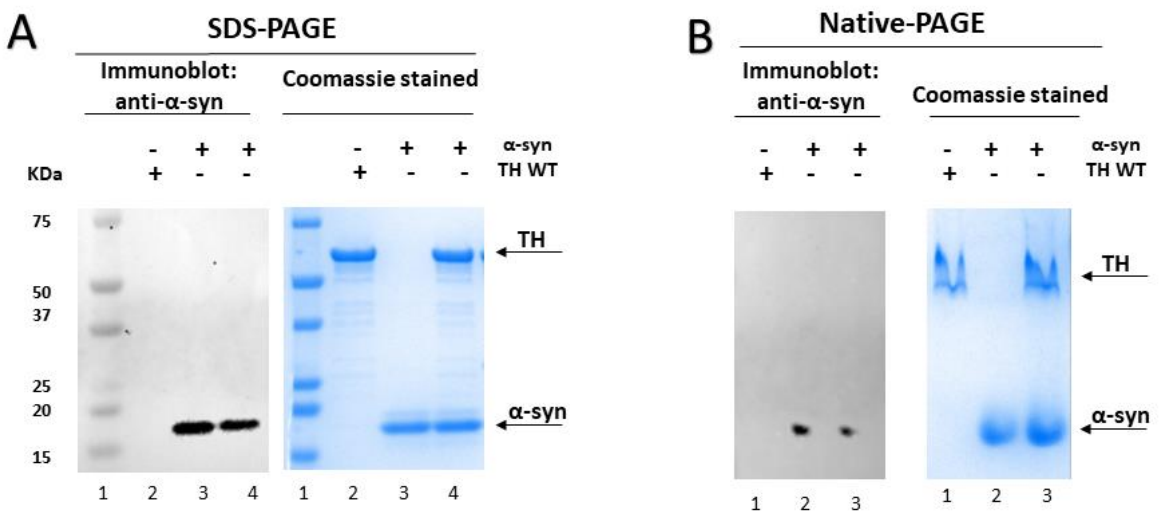

Figure 15: Analysis of the TH WT: α-syn complex formation by SDS-PAGE or Native-PAGE, with subsequent Coomassie staining and anti-α-syn immunoblotting. A) Anti-α-syn immunoblotted and Coomassie stained denaturating SDS-PAGE analysis of the samples. Lane 1: Precision Plus™ Dual Color Standard; lane 2: TH WT control; lane 3: α-syn control; lane 4: TH WT and α-syn mix. B) Anti-α-syn immunoblotted and Coomassie stained Native-PAGE analysis of the samples. Lane 1: Precision Plus™ Dual Color Standard; lane 2: TH WT control; lane 3: α-syn control; lane 4: TH WT and α-syn mix.

4.2.2 Crosslinking

Because both SEC-MALS and Native PAGE are techniques that can only detect tight and sustained protein interactions that do not dissociate as the complex migrates through the matrices of columns or gels, crosslinking experiments were performed to capture a possible weak or transient interaction between the proteins. Crosslinkers covalently link interacting proteins together and thus crosslinked complexes can even withstand denaturing conditions such as extreme heat and the presence of reducing agents. Therefore, results of the crosslinking reactions were analysed by SDS-PAGE.

The SDS-PAGE analysis *(Figure 16)* includes both controls of the proteins TH WT, TH Ser31Glu and α-syn that have gone through crosslinking reactions themselves alone (lanes 2-4) and controls that have not been subjected to crosslinking reactions (lanes 7-9). Lanes 5 and 6 contains samples from the crosslinking reactions between α-syn and TH WT or TH Ser31Glu respectively. In lanes 3-4, bands can be observed at ~120 kDa, ~150 kDa, ~250 kDa, that are not consistent with the sizes of the controls without crosslinkers, indicating the formation of crosslinked oligomers. These bands

are consistent with the theoretical sizes of the TH dimer, trimer, and tetramer at 112 kDa, 168 kDa and 224 kDa respectively, showing that a small proportion of the TH WT and TH Ser31Glu samples were crosslinked, even though the majority of the sample remained unchanged by the crosslinkers in the monomeric form. In lanes 5 and 6, with samples containing α-syn and TH WT or TH Ser31Glu, we would expect to see shifts in the bands when comparing them to the controls if the crosslinking between either of the TH variants and α-syn had been successful. However, no such shift was observed, indicating that there was no complex formation between α-syn and TH at these conditions. Due to time limitations further optimization of these cross-linking experiments were not performed, and we instead went on to study the possible interaction between TH and α-syn using BLI which is ideal to study transient interactions.

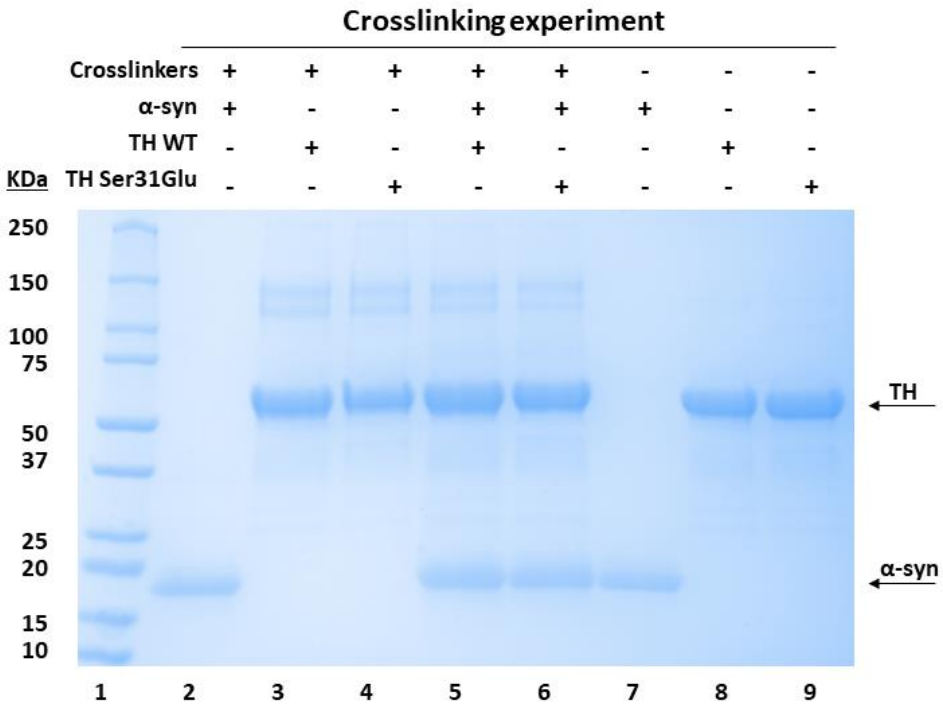

Figure 16: SDS-PAGE analysis of crosslinking reaction samples. Lane 1: Precision Plus™ Dual Color Standard; lane 2: Crosslinked α-syn control; lane 3: Crosslinked TH WT control; lane 4: Crosslinked TH Ser31Glu control; lane 5: TH WT and α-syn crosslinking reaction; lane 6: TH Ser31Glu and α-syn crosslinking reaction; lane 7: α-syn control (no crosslinkers); lane 8: TH WT control (no crosslinkers); lane 9: TH Ser31Glu control (no crosslinkers).

4.2.2 Bio-layer interferometry

BLI is a technique that allows the real time measurement of the affinity between a protein-protein interaction and can also be used to study weak or transient interactions. In our BLI-assays, biotinylated TH is immobilized on streptavidin biosensors and allowed to interact with α-syn. Since we hypothesize that α-syn may have a specific interaction with TH, biotinylated phenylalanine hydroxylase (PAH), a non-neuronal enzyme with a similar size and shape as TH, and for which interaction with α-syn has not been reported, was also immobilized on a streptavidin sensor and allowed to interact with α-syn as a negative control.

The BLI sensorgram from this assay is shown in *Figure 17*, where the binding response recorded by the sensor was plotted over time. Although the binding curve for TH and α-syn (red) seems to indicate binding between the two proteins, a similar binding curve was obtained from the negative control with PAH immobilized on the sensor (blue), indicating that the signal may be due to unspecific binding of α-syn to the sensor or similar binding to PAH. As these results, also seen in the context of the previous data, have not suggested specific direct binding between recombinant TH and α-syn and because of the low signal to noise ratio, we did not proceed with further BLI analyses to test the affinity between TH and α-syn.

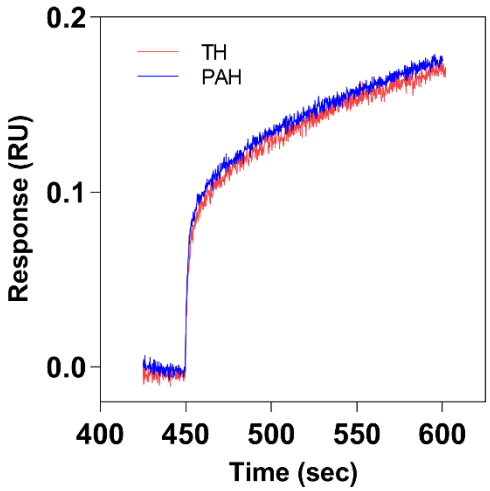

Figure 17: Analysis of binding of TH WT and α-syn using BLI. The binding response measured between TH WT and α-syn (red) was similar to the response measured between the negative control PAH and α-syn (blue), indicating non-specific binding of α-syn to the streptavidin biosensor.

4.3 Investigating the effect of different binding partners of tyrosine hydroxylase on dopamine feedback inhibition

The regulation of TH by DA controls L-Dopa and DA synthesis and is crucial for catecholamine homeostasis. The mechanism by which DA inhibits TH involves the induction of the interaction between the N-terminal α-helix (residues 39-58) and the catalytic domain, immobilizing the α-helix and locking DA in the active site (5) (*Figures 3 and 4*). This regulatory mechanism is particularly important, as elevated levels of DA and catecholamines are neurotoxic (58). It is therefore relevant to study the interplay between the regulatory protein partners and DA, particularly by investigating how dopamine influences the binding affinity of the proteins and how these alter the feed-back inhibition by DA. The partners selected for the binding studies by BLI included the co-chaperone DNAJC12 and the regulatory 14-3-3ζ protein. As previous experiments had not indicated a specific direct interaction between TH and α-syn (see above), this protein was not included in further binding assays by BLI, but we in any case measured if α-syn had any influence of the inhibition of TH activity by DA.

4.3.1 Bio-layer interferometry

BLI assays were performed to investigate the effect of DA on the affinity between TH and selected binding partners. The assays were done by using a concentration series of DNAJC12 or 14-3-3ς and then subsequently measuring the amount of binding with immobilized TH on the sensor at each concentration, both in the presence or absence of DA. The average binding responses recorded from separate triplicate experiments were plotted against the concentration of binding partner used. The dissociation constant (K_d)-values were then calculated from these plots and reported as mean ± standard error of the mean.

Figure 18A shows a representative sensorgram from the association and dissociation steps for the interaction between TH WT and DNAJC12. The sensorgram shows an increasing signal that stabilises towards the end of the association step, this signal signifies the interaction between TH WT and DNAJC12. The subsequent decrease in signal corresponds well with the disassociation of the proteins.

The results for the BLI-assays between TH WT and DNAJC12, with and without DA, are shown in *Figure 18B*. Similar K_d-values were derived for both conditions, with K_d-values of 131.0 ± 18.8 nM when DA was not present, and 124.7 ± 22.7 nM when DA was present. The difference in K_d-values was not deemed significant.

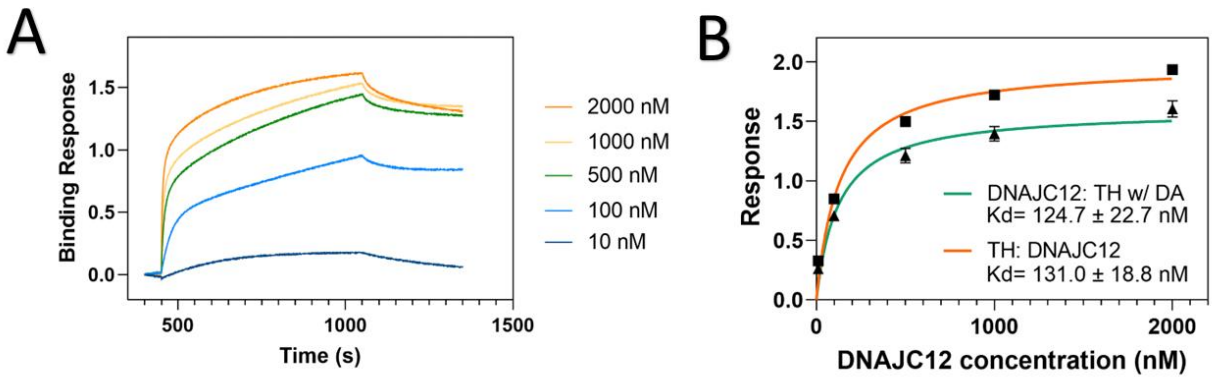

Figure 18: Analysis of binding between TH WT and DNAJC12, with and without DA present, by BLI. A) Representative sensorgrams of the reactions (using 2000 nM (orange), 1000 nM (yellow), 500 nM (green), 100 nM (light blue), 10 nM (dark blue) concentrations). B) Binding curves obtained from the fitting of triplicates to a one site binding (hyperbola) nonlinear regression model, with response plotted versus DNAJC12 concentration. The binding curve for the assay with DA in green (R^2=0.9630) and without DA in orange (R^2=0.9731).

Figure 19A shows an excerpt of a sensorgram from the association and dissociation steps for the for the interaction between TH pSer19 and 14-3-3ζ. The sensorgram shows a steep increase in signal that stabilises during the association step showing the binding of TH pSer19 and 14-3-3ζ. After the association step, one can observe a quick decrease in signal, signifying the disassociation of the proteins.

The binding curves for the BLI-assays between TH pSer19 and 14-3-3ζ, with and without DA, are shown in *Figure 19B*. The K_d-values obtained from these assays were 736.5 ± 108.8 nM with DA present, and 368.4 ± 103.1 nM without DA. The difference in K_d-values was not deemed significant. The K_d-value for the affinity between TH pSer19 and 14-3-3ζ without DA present, is higher than the earlier reported K_d-value of ~55.6 nM for mammalian 14-3-3ζ, measured by SPR (59). The deviation may be due to factors such as differences in the expression of the proteins, the

fact that we immobilised TH in the assay instead of 14-3-3ζ as in the previous study (59), or the use of the method BLI instead of surface plasmon resonance.

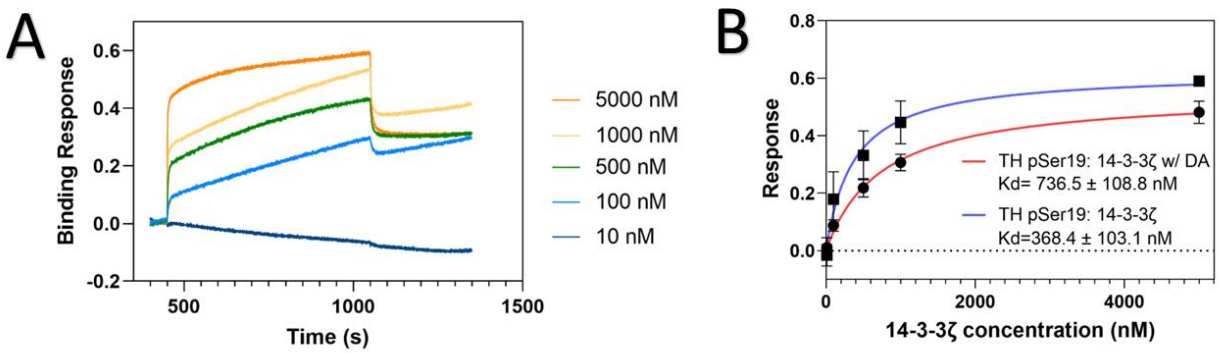

Figure 19: Analysis of binding between TH pSer19 and 14-3-3ζ, with and without DA present, by BLI. A) Representative sensorgrams of the reactions (using 5000 nM (orange), 1000 nM (yellow), 500 nM (green), 100 nM (light blue), 10 nM (dark blue) concentrations). B) Binding curves obtained from the fitting of triplicates to a one site binding (hyperbola) nonlinear regression model, with response plotted versus 14-3-3ζ concentration. The binding curve for the assay with DA in red (R^2=0.9722) and the assay without DA in blue (R^2=0.9170).

4.3.2 Enzymatic assays

Enzymatic assays were performed to determine whether the binding partners 14-3-3ζ and DNAJC12, as well as the potential binding partner α-syn affected the feedback inhibition of TH by DA. To ensure that the reaction time for the assays was within the linear range, enzymatic assays were performed for TH WT and TH Ser31Glu, measuring the activity after allowing the reaction to go on for 0-, 2-, 5-, 10-, and 15-min, as shown in *Figure 20*. *Figure 20A and 20B* show that the activity is linear for both TH WT and TH Ser31Glu within the time range of 0-15 min, including the chosen reaction time of 5 min for the performed assays.

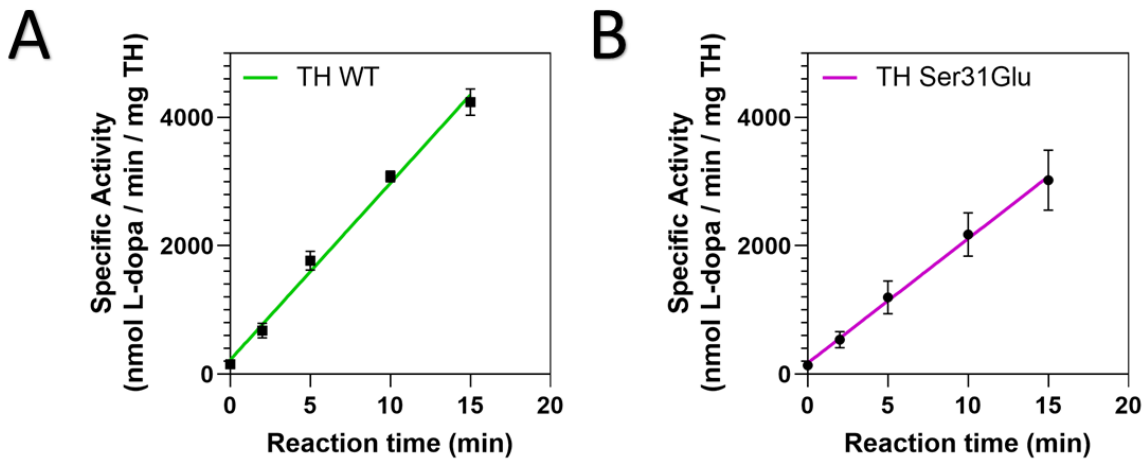

Figure 20: Enzymatic assays performed on TH WT and TH Ser31Glu, at variable reaction times, to confirm linearity. Graphs obtained from the fitting of triplicates to a simple linear regression model, with specific activity versus reaction time. A) Specific activity of TH WT as a function of time, R^2=0.9510. B) Specific Activity of TH Ser31Glu as a function of time, R^2=0.9892.

Then, further enzymatic assays were performed to determine the effect of 14-3-3ζ and DNAJC12 on inhibition by DA of TH pSer19 and TH WT, respectively. The effect of α-syn was assayed with both TH WT and TH Ser31Glu. For each protein, experiments were performed both with and without the selected binding partner in the mix with a concentration of TH in the assay of 18 nM (*Figure 21A-D*). For DNAJC12, we performed two types of assays, one by mixing TH WT and DNAJC12 at the start of the enzymatic reaction and by using DNAJC12 and TH WT purified as a DNAJC12: TH complex by SEC (*Figure 21C*).

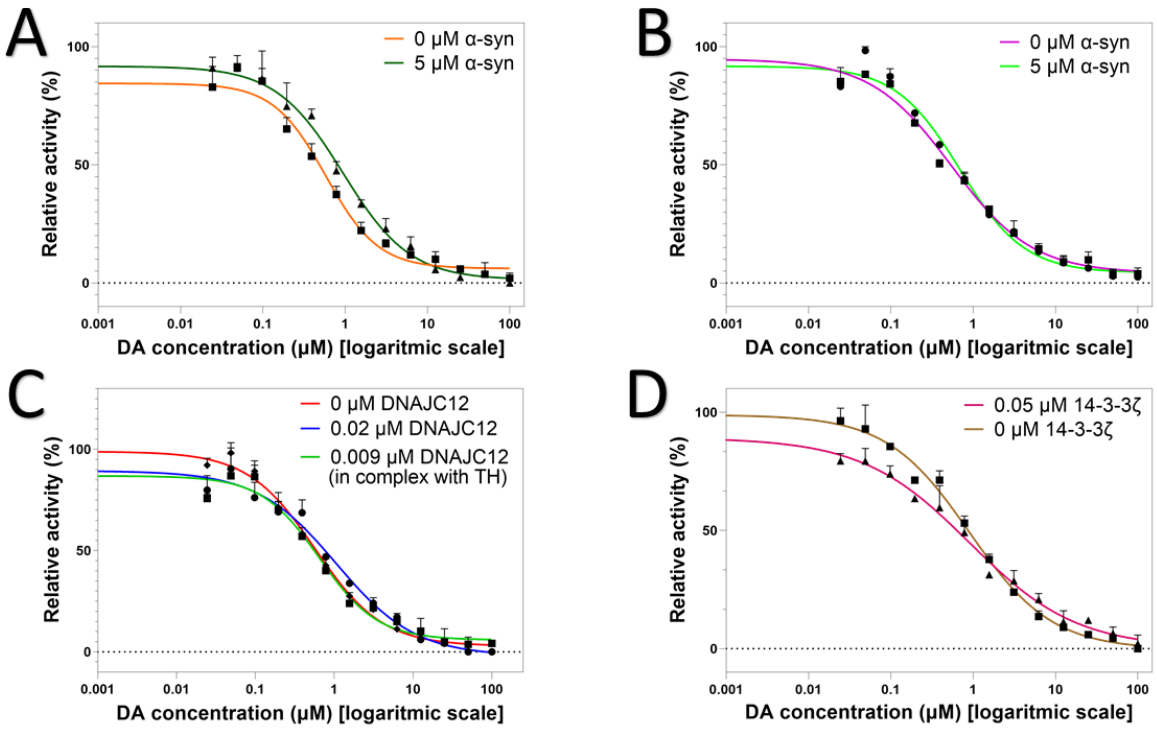

Figure 21: IC_{50} curves showing the inhibition of DA on TH activity, and the effects of known TH binding partners. IC_{50} curves obtained from the fitting of triplicates to a four-parameter nonlinear regression model, with relative activity plotted versus DA concentration. A) IC_{50}-curves for the DA inhibition of TH WT with and without α-syn. B) IC_{50}-curves for the DA inhibition of TH Ser31Glu with and without α-syn. C) IC_{50}-curves for the DA inhibition of TH WT with and without DNAJC12, and for the preformed TH: DNAJC12 complex (see text). D) IC_{50}-curves for the DA inhibition of TH pSer19 with and without 14-3-3ζ.

The IC_{50}-value were determined by plots containing 14 data points. Each point value represents the average of three replicate samples. Each IC_{50}-assay was repeated twice. In *Figure 22*, the results from these assays are reported as the average value with the standard error of the mean. The IC_{50}-values significantly different from the "0 µM α-syn (TH WT)" experiment are marked with *.

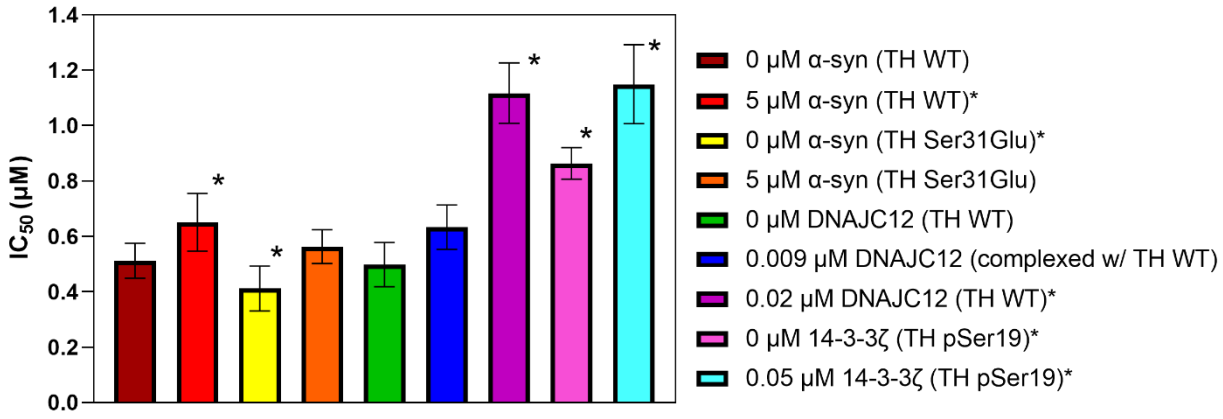

Figure 22: IC_{50}-values for the inhibition of TH WT, TH pSer19 and TH Ser31Glu by DA, in the presence and absence of selected binding partners. The IC_{50}-values significantly different from the "0 µM α-syn (TH WT)" experiment are marked with *.

Earlier reported IC_{50}-values for the inhibition of unphosphorylated TH WT by DA (5) agree with the IC_{50} values obtained by us for TH WT with IC_{50} values of 0.512 ± 0.063 µM and 0.498 ± 0.080 µM in the experiments named "0 µM α-syn (TH WT)" and "0 µM DNAJC12 (TH WT)" respectively. TH pSer19 (named 0 µM 14-3-3ζ (TH pSer19)) had an IC_{50} value of 0.863 ± 0.057 µM, whilst the phospho-mimicking TH Ser31Glu variant (named 0 µM α-syn (TH Ser31Glu)) had an IC_{50} value of 0.411 ± 0.081 µM. The inhibition of TH by DA thus shows that when TH is phosphorylated at Ser19, the inhibition by DA is decreased compared to the unphosphorylated WT, whilst the DA inhibition of the phospho-mimicking TH Ser31Glu variant appears to be slightly stronger than for TH WT.

As for the impact of α-syn on the DA inhibition of TH variants, the 5 µM α-syn (TH WT) and the 5 µM α-syn (TH Ser31Glu) assays each gave IC_{50}-values of 0.651 ± 0.104 µM and 0.563 ± 0.061 µM, respectively. The presence of α-syn therefore seems to constitute a trend with higher IC_{50}, and thus less DA inhibition, both for TH WT and for TH Ser31Glu.

In the 0.02 µM DNAJC12 (TH WT) assay, where DNAJC12 was added by itself prior to incubation, we obtained an IC_{50}-value of 1.117 ± 0.109 µM. When the purified DNAJC12-TH WT complex was assayed, an IC_{50}-value of 0.633 ± 0.080 µM was acquired. The difference in obtained IC_{50}-values, might be due to the difference in the amount DNAJC12 available in the assay. For DNAJC12 that already was complexed with TH, the inhibition by DA is slightly lower than when

DNAJC12 is not present in the mix. When excess DNAJC12 is added separately on the other hand, there is a significant two-fold increase in the IC_{50}-value.

The TH pSer19 accounted for an already raised IC_{50}-value when compared to unphosphorylated TH WT. With the added presence of 14-3-3ζ, the IC_{50} was further raised to a value of 1.149 ± 0.143 μM, accounting for a two-fold increase compared to unphosphorylated TH.

5. Discussion

The synthesis of DA and other catecholamines by AAAHs is vital for several physiological functions. DA is particularly important for its role in motor control, cognitive function and the brain reward system (3). DA is also, to some degree, responsible for the regulation of its own biosynthesis through an inhibitory feedback mechanism on the rate limiting step of the metabolic pathway, the conversion of L-Tyrosine to L-Dopa by the enzyme TH.

Biological processes are rarely the result of a single protein working alone, and protein-protein interactions therefore play an important role, for instance, in metabolic pathways. Among other things, these interactions contribute to the regulation of enzymes (60). In addition to DA, TH has previously been shown to interact with the co-chaperone DNAJC12 (35), the regulatory protein 14-3-3ζ (2) and the neuronal protein α-syn (16).

The aim of this master thesis was to understand the mechanisms behind the complex formation between TH and α-syn, to better characterised interactions of DNAJC12 and 14-3-3ζ with TH, and then to further investigate the effect of these protein-protein interactions on the inhibitory feedback mechanism by DA. A better understanding of the interplay between these proteins and DA can contribute to better understanding of the DA synthesis pathway, and in time, aid in creating the basis for the development of important therapies to treat DA deficiency disorders, such as PD.

5.1 The interaction between tyrosine hydroxylation and α-synuclein

Initial experiments done to study the interaction between α-syn and TH using SEC-MALS *(Figure 14)*, SDS-PAGE and Native PAGE coupled with immunoblotting *(Figure 15)* gave no indication of a direct interaction between α-syn and TH WT or the phospho-mimicking variant TH Ser31Glu. These results do not correspond with previous studies which have identified an interaction between TH and α-syn by co-immunoprecipitation (co-IP) (31) and by proximity ligation assay (PLA) (16).

A clear difference of how the previous co-IP experiments were performed compared to our SEC-MALS, SDS-PAGE and Native PAGE experiments, however, is the use of rat brain homogenate as input to co-IPs. By immunoprecipitating natively expressed proteins directly from brain homogenate the proteins of interest have been expressed in their natural environment together with

other potential binding partners, or with any PTMs present that may be necessary for protein complex formation. co-IP allows the pull-down of full protein complexes, and thus if specific modification in e.g. α-syn or another protein is required to mediate the interaction between TH and α-syn, positive results would have been observed with co-IP but not in our *in vitro* studies that only use the two proteins. On the other hand, a disadvantage by co-IPs is the possibility of co-immunoprecipitating proteins that are not directly forming complexes, thus one can easily have false positives. PLA, is a powerful in-cell technique that allows the detection of proteins in proximity of each other (< 40nm). The PLA data therefore indicates a proximity for TH and α-syn in the cell but does not prove a direct interaction. Again, as the proteins studied here are in their native state in the cell, these proteins may also have modifications or other binding partners that we have not accounted for in our *in vitro* assays.

To identify the other proteins that may be present in an endogenous TH-α-syn-complex, a co-IP experiment followed by a mass spectrometry (MS) analysis could help to determine components that would be necessary to reconstitute the complex *in vitro*.

Altogether, TH and α-syn do not appear to form a protein-protein complex in vitro. This could be due to the lack of the correct PTMs, proximity to membranes (as the binding of α-syn to membranes is known to change its conformation), other factors in the cellular environment, or simply that they do not interact directly after all.

5.2 Investigating a possibly weak or transient interaction between tyrosine hydroxylase and α-synuclein

The results from our initial studies did not indicate a direct interaction between TH and α-syn. However, if the interaction is weak or transient, as earlier suggested for the interaction between Ser31 phosphorylated TH and α-syn (16), the interaction may not be strong enough for the protein-protein complex to be detected using SEC-MALS and Native PAGE coupled with immunoblotting, as low-affinity or transient complexes will dissociate when migrating through a column or a gel.

Our crosslinking experiments were only partially successful in crosslinking TH monomers in the tetrameric protein, suggesting that further optimization of conditions is necessary to apply the

technique to investigate a transient interaction. This experiment could for instance have been optimized, either by using other crosslinkers, by incubating for a longer time or by changing reaction conditions such as reaction buffer or pH, but due to time limitations, this was not performed.

Upon further investigation of the putative TH: α-syn interaction by BLI *(Figure 17)*, another method well suited to catch weak or transient interactions, there was still no indication of direct interaction between α-syn and TH. Although the results from the BLI *(Figure 17)* indicated binding at first, similar binding responses were recorded from the negative control (PAH), indicating that the signal is due to non-specific binding of α-syn to the streptavidin sensors or to a similar interaction with PAH. To be able to draw information about the TH: α-syn interaction from this method, one must first reduce non-specific binding and thus the ambient noise. A strategy to reduce the ambient noise is to reverse the experiment, in this case by immobilising α-syn instead of TH to the sensor. Alternatively, other similar methods like Surface Plasmon Resonance or Isothermal Titration Calorimetry that can quantify binding kinetics could also be used. It should also be mentioned that α-syn has been reported to be constitutively acetylated at the N-terminal (61), a feature lacking from the recombinant protein used in all of our experiments, and so it may be advantageous to N-acetylate α-syn prior to doing these experiments.

A more unconventional approach to study the interaction between TH and α-syn and overcome the challenge of studying low-affinity or transient complexes in their native states could be the use of proximity-based biotin identification which has gained increasing popularity recently for allowing the identification of components of transient complexes in cells. In this technique, a target cell line is transfected with a plasmid that encodes for a promiscuous biotin ligase fused to the protein of interest, in our case either TH or α-syn, and the cells are also supplemented with biotin in the media (62).

When proteins bind to the target protein, the ligase biotinylates the interacting partners. These interacting partners can then be purified using streptavidin beads and the samples are analyzed by MS. While this technique is quite stringent as it requires a proximity of <10 nm, there is always a possibility of identifying proteins that are just close to the target protein in the cell but do not necessarily interact with it or those that have affinity to the ligase itself. Thus, apart from running

replicates, another culture that is transfected with a plasmid encoding only the biotin ligase is also analyzed in parallel to reduce the noise in the data (62).

All in all, we did not obtain any indication of a direct interaction between TH and α-syn through crosslinking or BLI. One reason can be that the interaction between the two proteins is indirect, rather than direct, as our methods are not suited to detect indirect associations. Another possibility, in the case of a direct interaction, is the lack of physiological conditions in our experiments, including any effector molecules, other binding partners and PTMs.

5.3 The effect of dopamine on the affinity between tyrosine hydroxylase and binding partners

As earlier mentioned, TH has been shown to exist in both an active and an DA-inhibited state. When inhibited by DA, TH is in its inactive state. Upon phosphorylation of the Ser40 residue the inhibition is lifted, and the active state induced (5). It was therefore reasonable to study whether the affinity between TH and the binding partners 14-3-3ζ and DNAJC12 is affected by the conformational change induced by DA and further down the line if DA inhibition is affected by protein complex formation.

The results from the BLI-assay between TH WT and DNAJC12 *(Figure 18)*, indicate that the interaction between TH WT and the co-chaperone is independent of the conformational change brought forward by DA. These results also go well with preliminary unpublished cryogenic electron microscopy (cryo-EM) data for the TH: DNAJC12 complex from our lab in collaboration with the Valpuesta lab in Madrid, showing that DNAJC12 binds around areas of the catalytic domains that do not appear to interfere with the conformational change involving the N-terminal regulatory helix that enters the active site upon DA binding (unpublished data).

As the main function of DNAJ proteins is to recognize and bind to their client proteins and cooperate with HSP70s to mediate client protein homeostasis, these results also imply that DNAJC12 will be able to recognize both DA-inhibited and active states. Previous work from the lab (39) has also shown the ability of DNAJC12 to delay TH aggregation, and thus with these BLI

results, it is reasonable to believe that DNAJC12 will protect TH from aggregation also in the DA-inhibited state.

The results from the BLI-assay between TH pSer19 and 14-3-3ζ *(Figure 19)* on the other hand, indicate that the binding partner discriminates between the DA-inhibited and active conformation of TH pSer19. The K_d-value for the affinity between TH pSer19 and 14-3-3ζ is higher with DA present, than without. This indicates that the presence of DA, and thus the conformational change towards the inhibited state of TH (5), weakens the interaction between the two proteins. Previous studies have shown that 14-3-3ζ binds the N-terminal domain of TH around pSer19 (2) (*Figure 8*) and that the binding of DA to TH moves the N-terminal α-helix (residue 39-58) to the catalytic domain (5) (*Figures 3 and 4*). Thus, our results indicate that the affinity of 14-3-3ζ for TH pSer19 increases when the N-terminal domain is free and detached from the active site. However, the difference was not deemed significant, and the experiments would have to further strengthen this hypothesis.

5.4 The effect of α-synuclein, DNAJC12 and 14-3-3ζ on inhibition of tyrosine hydroxylase by dopamine

DA is considered the master regulator of TH activity, and thus also of DA synthesis. To assess whether protein complex formation between TH and binding partners might affect the DA feedback mechanism we determined IC_{50} values for DA inhibition in the presence of α-syn, 14-3-3ζ and DNAJC12.

The results from our activity studies did not indicate that α-syn affects the regulation of TH by DA. Although the results from the enzymatic assays with α-syn *(Figure 22)* shows a slightly elevated IC_{50}-value, both for the TH WT and TH Ser31Glu variants, one should also keep in mind that we have previously not been able to characterise the interaction between TH and α-syn. α-syn has also been shown earlier to bind directly to DA(33) and it is possible that this interaction could lead to the reduction of free DA in the reaction mix, thus explaining the slightly elevated IC_{50}-values.

In the activity assays with DNAJC12, the results *(Figure 22)* showed an elevated IC_{50}-value of DA inhibition, suggesting that in addition to its role as co-chaperone of TH (39) DNAJC12 also regulates TH activity, leading to higher activity at equal DA concentrations in the media, and

possibly at intracellular conditions. Although DNAJC12 binding appears to affect the feedback mechanism by DA on TH, DA is still able to act as a strong regulator of TH activity. An earlier study has indicated that DNAJC12 slows down the aggregation of TH, independent of binding to HSP70 chaperones (39). Apart from this, unpublished results from our lab using differential scanning fluorimetry show that the presence of DNAJC12 slightly increases the melting temperature of TH, indicating that DNAJC12 increases the conformational stability of TH. This stabilizing effect could potentially contribute to the slight increase in the IC_{50}-value for DA inhibition.

For the binding partner 14-3-3ζ, results from the enzymatic assay *(Figure 22)* indicate that the phosphorylation of the Ser19 residue of TH reduces the inhibition by DA, and that the subsequent binding of 14-3-3ζ to TH pSer19 further reduces DA inhibition. The change in both cases was deemed significant. Although the change in IC_{50}-value appears small, the two-fold change is physiologically important as it gives a potential doubling of DA at the nerve terminals. Just as phosphorylation of the Ser40 residue in the α-helix (residues 39-58) is known to fully lift the DA inhibition (5), the phosphorylation of the Ser19 residue could potentially similarly weaken the affinity between the N-terminal and the catalytic domain, but to a much lesser extent, as the phosphorylated residue is not located in the α-helix. The interaction of 14-3-3ζ with TH in this N-terminal region could thus further weaken the affinity between the α-helix and the catalytic domain in a similar manner, and thus reducing the effect of the feedback inhibition by DA.

These *in vitro* studies come with both advantages and disadvantages. An advantage with our *in vitro* studies is the possibility to regulate components in the reaction mix, thus making it easier to ascribe the observed affects to a specific molecule in an *in vitro* assay, but at the same time a disadvantage is a lack of physiologically relevant conditions and environments (PTMs, binding partners, etc) that may be essential for the studied processes. Despite the disadvantages of *in vitro* studies of such complex systems our results represent a step forward towards a better understanding of interplay between TH, DA, and binding partners and of how TH regulation by DA can be affected by protein-protein interactions in the cell.

6. Conclusion

The aim of this thesis was to further elucidate the interaction between TH and α-syn and gain further insight into the regulation of TH through the inhibitory feedback mechanism by DA by studying how α-syn, DNAJC12 and 14-3-3ζ affects this inhibition. Moreover, the thesis has provided expertise in a series of relevant techniques to study biomolecular interactions and their interplay with the feed-back inhibition of TH by DA. In this work we obtained pure, recombinant α-syn, TH WT and TH Ser31Glu which allowed us to initiate in vitro studies. We were not able to show a direct interaction between α-syn and TH and our results can indicate that the interaction might be indirect or that other environmental factors or PTMs are needed for complex formation to occur. Affinity and enzymatic activity assays gave further insight into how TH binding partners affect the feedback inhibition by DA. The affinity between TH and DNAJC12 is unaffected by the presence of DA, and though the feedback inhibition by DA appears affected by the presence of DNAJC12, this may be explained by DNAJC12 ability to stabilize TH and decrease the enzyme dynamics at play for the conformational change associated with DA-inhibition. This suggests that DA and DNAJC12 are both able to interact with and regulate TH simultaneously. Finally, the affinity between 14-3-3ζ and TH pSer19 was decreased by the presence of DA, and the feedback inhibition by DA was weakened by Ser19 phosphorylation and further by the binding of 14-3-3ζ, likely due to the N-terminals involvement in both processes.

7. Future Perspectives

The elucidation of the protein-protein interaction between α-syn and TH is important for understanding the function of the complex and its role in the dopamine synthesis. The TH:α-syn complex has previously been identified by co-immunoprecipitation (31). Coupling mass spectrometry to co-immunoprecipitation using either TH or α-syn as bait would be a good approach to identify whether there are other proteins or PTMs required for binding between TH and α-syn, thus allowing further characterisation of the protein-protein complex.

α-syn has also been reported to be constitutively acetylated at the N-terminal *in vivo*. This PTM could prove important for the interaction between TH and α-syn. N-terminal acetylation results in a reduced positive charge at the N-terminal, which would leave α-syn better suited for hydrophobic binding. Binding studies including N-terminal acetylated α-syn would help determine the importance of this modification for the interaction between TH and α-syn.

Further characterisation of the complex formation between TH and α-syn is also important for the study of the effect of α-syn on the DA feedback inhibition. As no interaction between TH and α-syn was demonstrated in this thesis, the lack of a complex formation could be expected for the enzymatic assays. Therefore, if the missing link of the TH: α-syn interaction were to be identified, the enzymatic assay should be repeated to elucidate a more physiologically relevant effect of α-syn on the DA feedback inhibition.

Furthermore, the BLI-assays and the enzymatic assays should be repeated to validate the accuracy of the observed effects for DNAJC12 and 14-3-3ζ on the inhibitory feedback mechanism by DA. Cryo-EM could be performed to obtain a model of DNAJC12 bound to TH inhibited by DA. Methods like proximity-based biotin identification could also prove valuable in further work with mapping other components in this complex formation, including weak affinity and transient complexes. Further insights into the network of interactions responsible for the regulation of TH can in time provide interesting drug targets allowing for the screening of compounds with the potential to regulate the DA synthesis through stabilization of protein-protein interactions.

Bibliography

1. Bezem MT, Baumann A, Skjærven L, Meyer R, Kursula P, Martinez A, et al. Stable preparations of tyrosine hydroxylase provide the solution structure of the full-length enzyme. Scientific Reports. 2016;6(1):30390.

2. Skjevik ÅA, Mileni M, Baumann A, Halskau Ø, Teigen K, Stevens RC, et al. The N-Terminal Sequence of Tyrosine Hydroxylase Is a Conformationally Versatile Motif That Binds 14-3-3 Proteins and Membranes. Journal of Molecular Biology. 2014;426(1):150-68.

3. Klein MO, Battagello DS, Cardoso AR, Hauser DN, Bittencourt JC, Correa RG. Dopamine: Functions, Signaling, and Association with Neurological Diseases. Cellular and Molecular Neurobiology. 2019;39(1):31-59.

4. German CL, Baladi MG, McFadden LM, Hanson GR, Fleckenstein AE. Regulation of the Dopamine and Vesicular Monoamine Transporters: Pharmacological Targets and Implications for Disease. Pharmacological Reviews. 2015;67(4):1005-24.

5. Bueno-Carrasco MT, Cuéllar J, Flydal MI, Santiago C, Kråkenes T-A, Kleppe R, et al. Structural mechanism for tyrosine hydroxylase inhibition by dopamine and reactivation by Ser40 phosphorylation. Nature Communications. 2022;13(1).

6. Hufton SE, Jennings IG, Cotton RGH. Structure and function of the aromatic amino acid hydroxylases. Biochemical Journal. 1995;311(2):353-66.

7. Fitzpatrick PF. Structural insights into the regulation of aromatic amino acid hydroxylation. Current Opinion in Structural Biology. 2015;35:1-6.

8. Nagatsu T, Nakashima A, Ichinose H, Kobayashi K. Human tyrosine hydroxylase in Parkinson's disease and in related disorders. Journal of Neural Transmission. 2019;126(4):397-409.

9. Waløen K, Kleppe R, Martinez A, Haavik J. Tyrosine and tryptophan hydroxylases as therapeutic targets in human disease. Expert Opinion on Therapeutic Targets. 2017;21(2):167-80.

10. Szigetvari PD, Muruganandam G, Kallio JP, Hallin EI, Fossbakk A, Loris R, et al. The quaternary structure of human tyrosine hydroxylase: effects of dystonia‐associated missense variants on oligomeric state and enzyme activity. Journal of Neurochemistry. 2019;148(2):291-306.

11. Pace CN, Vajdos F, Fee L, Grimsley G, Gray T. How to measure and predict the molar absorption coefficient of a protein. Protein Science. 1995;4(11):2411-23.

12. Teigen K, McKinney JA, Haavik J, Martinez A. Selectivity and Affinity Determinants for Ligand Binding to the Aromatic Amino Acid Hydroxylases. Current Medicinal Chemistry. 2007;14(4):455-67.

13. Goodwill KE, Sabatier C, Marks C, Raag R, Fitzpatrick PF, Stevens RC. Crystal structure of tyrosine hydroxylase at 2.3 Å and its implications for inherited neurodegenerative diseases. Nature Structural Biology. 1997;4(7):578-85.

14. Skjærven L, Teigen KE, Martínez A, editors. Structure-Function Relationships in the Aromatic Amino Acid Hydroxylases Enzyme Family: Evolutionary Insights2014.

15. Gordon SL, Quinsey NS, Dunkley PR, Dickson PW. Tyrosine hydroxylase activity is regulated by two distinct dopamine-binding sites. Journal of Neurochemistry. 2008;106(4):1614-23.

16. Jorge-Finnigan A, Kleppe R, Jung-Kc K, Ying M, Marie M, Rios-Mondragon I, et al. Phosphorylation at serine 31 targets tyrosine hydroxylase to vesicles for transport along microtubules. Journal of Biological Chemistry. 2017;292(34):14092-107.

17. Obšilová V, Šilhan J, Bouřa E, Teisinger J, Obšil T. 14-3-3 proteins: a family of versatile molecular regulators. Physiological Research. 2008;57:S11-S21.

18. Maroteaux L, Campanelli J, Scheller R. Synuclein: a neuron-specific protein localized to the nucleus and presynaptic nerve terminal. The Journal of Neuroscience. 1988;8(8):2804-15.

19. Burré J, Sharma M, Südhof TC. Cell Biology and Pathophysiology of α-Synuclein. Cold Spring Harbor Perspectives in Medicine. 2018;8(3).

20. Jakes R, Spillantini MG, Goedert M. Identification of two distinct synucleins from human brain. FEBS Letters. 1994;345(1):27-32.

21. Meade RM, Fairlie DP, Mason JM. Alpha-synuclein structure and Parkinson's disease – lessons and emerging principles. Molecular Neurodegeneration. 2019;14(1).

22. Huang M, Wang B, Li X, Fu C, Wang C, Kang X. α-Synuclein: A Multifunctional Player in Exocytosis, Endocytosis, and Vesicle Recycling. Front Neurosci. 2019;13:28-.

23. Stefanis L. -Synuclein in Parkinson's Disease. Cold Spring Harbor Perspectives in Medicine. 2012;2(2):a009399-a.

24. Dufty BM, Warner LR, Hou ST, Jiang SX, Gomez-Isla T, Leenhouts KM, et al. Calpain-Cleavage of α-Synuclein. The American Journal of Pathology. 2007;170(5):1725-38.

25. Emamzadeh F. Alpha-synuclein structure, functions, and interactions. Journal of Research in Medical Sciences. 2016;21(1):29.

26. Bussell R. Helix periodicity, topology, and dynamics of membrane-associated -Synuclein. Protein Science. 2005;14(4):862-72.

27. Bernal-Conde LD, Ramos-Acevedo R, Reyes-Hernández MA, Balbuena-Olvera AJ, Morales-Moreno ID, Argüero-Sánchez R, et al. Alpha-Synuclein Physiology and Pathology: A Perspective on Cellular Structures and Organelles. Front Neurosci. 2020;13.

28. Kim WS, Kågedal K, Halliday GM. Alpha-synuclein biology in Lewy body diseases. Alzheimer's Research & Therapy. 2014;6(5-8).

29. Bisaglia M, Trolio A, Bellanda M, Bergantino E, Bubacco L, Mammi S. Structure and topology of the non-amyloid-β component fragment of human α-synuclein bound to micelles: Implications for the aggregation process. Protein Science. 2006;15(6):1408-16.

30. Ulmer TS, Bax A, Cole NB, Nussbaum RL. Structure and Dynamics of Micelle-bound Human α-Synuclein. Journal of Biological Chemistry. 2005;280(10):9595-603.

31. Perez RG, Waymire JC, Lin E, Liu JJ, Guo F, Zigmond MJ. A Role for α-Synuclein in the Regulation of Dopamine Biosynthesis. The Journal of Neuroscience. 2002;22(8):3090-9.

32. Cartier EA, Parra LA, Baust TB, Quiroz M, Salazar G, Faundez V, et al. A Biochemical and Functional Protein Complex Involving Dopamine Synthesis and Transport into Synaptic Vesicles. Journal of Biological Chemistry. 2010;285(3):1957-66.

33. Mor DE, Tsika E, Mazzulli JR, Gould NS, Kim H, Daniels MJ, et al. Dopamine induces soluble α-synuclein oligomers and nigrostriatal degeneration. Nature Neuroscience. 2017;20(11):1560-8.

34. Angelova DM, Jones HBL, Brown DR. Levels of α - and β - synuclein regulate cellular susceptibility to toxicity from α - synuclein oligomers. The FASEB Journal. 2018;32(2):995-1006.

35. Anikster Y, Haack TB, Vilboux T, Pode-Shakked B, Thöny B, Shen N, et al. Biallelic Mutations in DNAJC12 Cause Hyperphenylalaninemia, Dystonia, and Intellectual Disability. The American Journal of Human Genetics. 2017;100(2):257-66.

36. Choi J, Djebbar S, Fournier A, Labrie C. The co-chaperone DNAJC12 binds to Hsc70 and is upregulated by endoplasmic reticulum stress. Cell Stress and Chaperones. 2014;19(3):439-46.

37. Blau N, Martinez A, Hoffmann GF, Thöny B. DNAJC12 deficiency: A new strategy in the diagnosis of hyperphenylalaninemias. Molecular Genetics and Metabolism. 2018;123(1):1-5.

38. Lee J, Hahn Y, Yun JH, Mita K, Chung JH. Characterization of JDP genes, an evolutionarily conserved J domain-only protein family, from human and moths. Biochimica et Biophysica Acta (BBA). 2000;1491(1-3):355-63.

39. Tai MDS. Understanding the interaction between the co-chaperone DNAJC12 and tyrosine hydroxylase [Master's thesis]. Bergen: University of Bergen; 2020.

40. Paulo RdAF, Mangone FR, Pavanelli AC, Simone AdBG, Nonogaki S, Cynthia ABdTO, et al. Gene expression profiling of triple-negative breast tumors with different expression of secreted protein acidic and cysteine rich (SPARC). Breast Cancer Management. 2018;7(2).

41. He H-L, Lee Y-E, Chen H-P, Hsing C-H, Chang IW, Shiue Y-L, et al. Overexpression of DNAJC12 predicts poor response to neoadjuvant concurrent chemoradiotherapy in patients with rectal cancer. Experimental and Molecular Pathology. 2015;98(3):338-45.

42. Uno Y, Kanda M, Miwa T, Umeda S, Tanaka H, Tanaka C, et al. Increased Expression of DNAJC12 is Associated with Aggressive Phenotype of Gastric Cancer. Annals of Surgical Oncology. 2019;26(3):836-44.

43. Yamauchi T, Nakata H, Fujisawa H. A new activator protein that activates tryptophan 5-monooxygenase and tyrosine 3-monooxygenase in the presence of Ca2+-, calmodulin-dependent protein kinase. Purification and characterization. Journal of Biological Chemistry. 1981;256(11):5404-9.

44. Ichimura T, Isobe T, Okuyama T, Yamauchi T, Fujisawa H. Brain 14-3-3 protein is an activator protein that activates tryptophan 5-monooxygenase and tyrosine 3-monooxygenase in the presence of Ca^{2+},calmodulin-dependent protein kinase II. FEBS Letters. 1987;219(1):79-82.

45. Foote M, Zhou Y. 14-3-3 proteins in neurological disorders. Int J Biochem Mol Biol. 2012;3(2):152-64.

46. Mhawech P. 14-3-3 proteins—an update. Cell Research. 2005;15(4):228-36.

47. Liu D, Bienkowska J, Petosa C, Collier RJ, et al. Crystal structure of the zeta isoform of the 14-3-3 protein. Nature. 1995;376(6536):191-4.

48. Dougherty MK, Morrison DK. Unlocking the code of 14-3-3. Journal of Cell Science. 2004;117(10):1875-84.

49. Kleppe R, Rosati S, Jorge-Finnigan A, Alvira S, Ghorbani S, Haavik J, et al. Phosphorylation Dependence and Stoichiometry of the Complex Formed by Tyrosine Hydroxylase and 14-3-3γ. Molecular & Cellular Proteomics. 2014;13(8):2017-30.

50. Gu Q, Cuevas E, Raymick J, Kanungo J, Sarkar S. Downregulation of 14-3-3 Proteins in Alzheimer's Disease. Molecular Neurobiology. 2020;57(1):32-40.

51. Neal CL, Yu D. 14-3-3ζ as a prognostic marker and therapeutic target for cancer. Expert Opinion on Therapeutic Targets. 2010;14(12):1343-54.

52. Neal CL, Yao J, Yang W, Zhou X, Nguyen NT, Lu J, et al. 14-3-3ζ Overexpression Defines High Risk for Breast Cancer Recurrence and Promotes Cancer Cell Survival. Cancer Research. 2009;69(8):3425-32.

53. Niemantsverdriet M, Wagner K, Visser M, Backendorf C. Cellular functions of 14-3-3ζ in apoptosis and cell adhesion emphasize its oncogenic character. Oncogene. 2008;27(9):1315-9.

54. Shen J, Person MD, Zhu J, Abbruzzese JL, Li D. Protein Expression Profiles in Pancreatic Adenocarcinoma Compared with Normal Pancreatic Tissue and Tissue Affected by Pancreatitis as Detected by Two-Dimensional Gel Electrophoresis and Mass Spectrometry. Cancer Research. 2004;64(24):9018-26.

55. Kråkenes T-A. Regulation of tyrosine hydroxylase activity by dopamine and α-synuclein [Master's thesis]. Bergen: University of Bergen; 2021.

56. Jakubec M, Bariås E, Furse S, Govasli ML, George V, Turcu D, et al. Cholesterol‐containing lipid nanodiscs promote an α‐synuclein binding mode that accelerates oligomerization. The FEBS Journal. 2021;288(6):1887-905.

57. Marsh JA, Forman-Kay JD. Sequence Determinants of Compaction in Intrinsically Disordered Proteins. Biophysical Journal. 2010;98(10):2383-90.

58. Biosa A, Arduini I, Soriano ME, Giorgio V, Bernardi P, Bisaglia M, et al. Dopamine Oxidation Products as Mitochondrial Endotoxins, a Potential Molecular Mechanism for Preferential Neurodegeneration in Parkinson's Disease. ACS Chem Neurosci. 2018;9(11):2849-58.

59. Toska K, Kleppe R, Armstrong CG, Morrice NA, Cohen P, Haavik J. Regulation of tyrosine hydroxylase by stress-activated protein kinases. Journal of Neurochemistry. 2002;83(4):775-83.

60. Rao VS, Srinivas K, Sujini GN, Kumar GNS. Protein-Protein Interaction Detection: Methods and Analysis. International Journal of Proteomics. 2014;2014:1-12.

61. Duce JA, Wong BX, Durham H, Devedjian J-C, Smith DP, Devos D. Post translational changes to α-synuclein control iron and dopamine trafficking; a concept for neuron vulnerability in Parkinson's disease. Molecular Neurodegeneration. 2017;12(1).

62. Sears RM, May DG, Roux KJ. BioID as a Tool for Protein-Proximity Labeling in Living Cells. Methods in Molecular Biology. 2019:299-313.